

NOTICE: this is the author's version of a work that was accepted for publication in *Precambrian Research*. Changes resulting from the publishing process, such as peer review, editing, corrections, structural formatting, and other quality control mechanisms may not be reflected in this document. Changes may have been made to this work since it was submitted for publication. A definitive version was subsequently published in *Precambrian Research*, Volume 158, Issues 1–2, 15 September 2007, Pages 79–92, <http://dx.doi.org/10.1016/j.precamres.2007.04.006>

Published in: *Precambrian Research*, 158 (2007), 79-92.

Ion-probe dating of 1.2 Ga collision and crustal architecture in the Namaqua-Natal Province of southern Africa.

*Åsa Pettersson¹, David H Cornell², Gabriel H F Moen³, Steven Reddy⁴, David Evans⁵

¹Earth Sciences Centre, Göteborg University, Box 460, SE-405 30 Göteborg; asap@gvc.gu.se, tel: +46(0)317862800, fax: +46(0)317862849

²Earth Sciences Centre, Göteborg University, Box 460, SE-405 30 Göteborg; cornell@gvc.gu.se

³Council for Geoscience, PO Box 775, Uppington 8800

⁴Department of Applied Geology, Curtin University, Bentley GPO Box U 1987, Perth, Western Australia 6845

⁵Geology and Geophysics Department, Yale University, P.O. Box 208109, New Haven, CT, 06520-8109 USA

Abstract

The Namaqua-Natal Province of southern Africa formed a part of the Kalahari craton, possibly linked to the ~1.0 Ga supercontinent Rodinia, but the timing of assembly and its positioning relation to other components is still debated. Thorough ion-probe zircon dating combined with strategic field observations in the tectonic front of a metamorphic belt can clarify some of these issues. In this study, the age of two “pre-tectonic” units, constrains the timing of collision and clarifies the role of the Koras Group as a tectonostratigraphic marker. The volcanosedimentary Wilgenhoutsdrif Group contains Archaean and Paleoproterozoic material, showing that it probably formed in a continental rift or a passive margin setting, before its involvement in the Namaqua collision event. At 1241 ± 12 Ma the Areachap island arc magmatism was in progress, followed by a collision event around 1200 Ma which at 1165 ± 10 Ma gave rise to migmatites in the island arc terrane. At the same time (1173 ± 12 Ma) in the adjoining Kaaien terrane the first sequence of Koras Group bimodal magmatism formed in a fault basin, invalidating the concept that this Group is a tectonostratigraphic marker of the end of tectonism in the whole Namaqua Province. A time of little activity followed, with yet another pulse of magmatism at 1100–1090 Ma, giving rise to a second sequence of sedimentation and volcanism in the Koras Group, as well as correlated intrusive rocks. This second pulse is not related to any significant regional deformation and may have

been thermally induced. It is in part coeval with the Umkundo large igneous province of the Kaapvaal and Zimbabwe Cratons. These formations preserve an important record for reconstructing Rodinia and our 1093 ± 7 Ma U-Pb age of the uppermost volcanic formation of the Koras Group, should be used as the age for the Kalkpunt Formation, frequently cited as a Kalahari Craton paleopole.

1 Keywords

2 Namaqua-Natal Province, Rodinia, U-Pb zircon, ion-probe dating, Koras Group, Kalahari
3 craton

4

5 **Introduction**

6 Collision events in the Namaqua sector have been assigned ages between 1.28 (Frimmel,
7 2004) and 0.9 Ga (Hoal, 1993), with many authors citing 1100 Ma (Thomas et al., 1996) and
8 most paleomagnetic syntheses start at 1100 Ma. The mid-Proterozoic supercontinent Rodinia
9 (Dalziel et al., 2000) included many ~1.0 Ga components now distributed over the globe. The
10 Namaqua sector of the Namaqua-Natal province of Southern Africa (Fig. 1) is one such
11 fragment, in which the timing of collision and subsequent events is poorly constrained.
12 Several workers, (Humphreys and Van Bever Donker, 1987; Stowe, 1986; van Zyl, 1981)
13 concluded that the north eastern part of the Namaqua sector is a structurally complex area
14 with at least one deformational phase prior to terrane assembly, and that several fold phases
15 developed in relation to Namaquan collision events, with the main event, here termed NF2.
16 This is evident in both the Areachap and Kaaian terranes. Stowe (1986) considered the area
17 we refer to as the Kaaian Terrane as a part of the Kgalagadi Province. Note that in Fig. 2 we
18 follow Thomas et al., (1994b) and Cornell et al. (2006), restricting the Kheis Province to east
19 of the Dabep thrust, following geochronological evidence that the main foliation in the region
20 between the Dabep thrust and Trooilopspan Shear Zone (here called the Kaaian Terrane) is
21 related to the Namaqua Orogeny.

22

23 The ion probe technique of zircon dating enables precise age determinations of rock-forming
24 events in complex metamorphic areas such as the Namaqua-Natal Province. Using
25 backscattered electron and cathodoluminescent images of zircon, distinct age domains such as
26 xenocrystic cores, oscillatory zoned magmatic areas and metamorphic rims can be identified

27 and metamict zones avoided by the ~30 micron ion beam. In this work we present a number
28 of precise ion probe dates for key formations and events in the NE marginal areas of the
29 Namaqua sector, which allow us to clarify the history before, during and after collision. We
30 show that the main collision event in this part of the Namaqua sector occurred after 1230 Ma
31 and before 1165 Ma.

32

33 The volcanosedimentary Koras Group in the Kaaien Terrane near Upington (Figs. 1, 2, and 3)
34 has been considered important due to its stratigraphic position in the Namaqua Front, being
35 regarded as undeformed and overlying highly deformed rocks of the Namaqua Province.

36 These relationships suggest that the Koras Group is younger than all deformation in the
37 collisional orogeny, possibly related to the formation of Rodinia (Gutzmer et al., 2000). This
38 concept led to the Koras Group being chosen as defining the top of the Mokolian Erathem of
39 the South African Committee for Stratigraphy (SACS) (1980), so that its age, although
40 variously defined at 1080, 1180 or 1123 Ma, is used as a chronostratigraphic boundary in
41 maps of the South African Geological Survey. Previous investigations include geochemistry
42 and several imprecise and contradictory whole rock or bulk zircon model age determinations
43 from 1.2 to 1.0 Ga, including 1.9 Ga xenocrysts (Table 1). Gutzmer et al. (2000) summarised
44 the earlier work and claimed that their precise 1171 ± 7 Ma ion probe Pb-Pb zircon age for a
45 Koras rhyolite resolved this topic. Palaeomagnetic data from the Koras Group provide
46 important points on apparent polar wander paths (Briden et al., 1979), but the precise age of
47 the formations sampled was not well known. In this work we confirm the age for one Koras
48 rhyolite, but also show that the Group represents at least 80 Ma of stratigraphic history. We
49 also demonstrate that the tectonostratigraphic relationships defining the end of Namaqua
50 deformation are valid only in the Kaaien Terrane, not in the terranes further west.

51 *Fig. 1*

52 *Table 1*

53

54 **Methods**

55 Zircons were separated from about 2 kg of each sample. The samples were crushed using a
56 swing mill and then sieved through 400 μ m. This material was panned by hand, heavy
57 minerals were dried and zircons were hand picked, mounted in epoxy and polished.
58 Cathodoluminescence and backscattered images were obtained for the individual zircon
59 grains, to identify age domains and to avoid cracks and metamict zones. All imaging for
60 samples with prefix DC was done using a Zeiss DSM 940 electron microscope at Gothenburg
61 University. A Cameca 1270 ion probe was used for U-Pb dating at the Nordsim facility in the
62 Swedish Natural History Museum in Stockholm, as described by Whitehouse et al. (1997;
63 1999). A ~30 micron oxygen ion beam was used and the NIST 91500 zircon standard was
64 used for calibration. Common Pb corrections samples run at Nordsim (prefix DC) assume a
65 present day Stacey & Kramers (1975) model average terrestrial Pb composition, based on the
66 observation that most common Pb is due to laboratory contamination. Sample S03-10 was
67 analysed with a SHRIMP instrument at Curtin University, Perth, Australia according to
68 (Nelson, 1997) using standard CZ3, common Pb correction with a Broken Hill type of
69 composition (Cummins & Richards, 1975) and cathodoluminescence imaging done at Curtin
70 University. Age calculations were made using the Isoplot 3 programme of Ludwig (1991;
71 1998). Uncertainties of age calculations are all given at the 2 σ level, ignoring decay constant
72 errors. Unless stated otherwise, all the dates reported in this work are ion probe zircon U-Pb
73 data.

74 The results are given in Table 2 and raw data in the supplementary data.

75 Mineral analysis of hornblende in DC0439, see Table 3, were done at Gothenburg University
76 on a Hitachi S-3400N Scanning electron microscope with an Oxford EDS system, and
77 pressure calculations in the programme by Tindle and Webb (1994).

78 *Fig. 2*

79 *Table 2*

80

81 **Wilgenhoutsdrif Group**

82 The upper part of the Wilgenhoutsdrif Group is made up of basaltic volcanic rocks which
83 contain preserved hyaloclastites and pillow lavas, with interbedded rhyolites, sandstones,
84 conglomerates, shales, and minor calcsilicates (Figs. 2 and 3). The group overlies the
85 Groblershoop Formation, a thrust package of metasedimentary quartz-mica schists which may
86 be as old as 1900 Ma (Theart et al., 1989) that probably represents a passive margin shelf
87 sequence on the western margin of the Kaapvaal Craton formed before the Kheis tectonism.
88 The Wilgenhoutsdrif Group is severely deformed and metamorphosed in the greenschist
89 facies. It shows two phases of deformation which according to Moen (1987; 1999), record the
90 Namaqua deformation history in this area. Geochemical data suggests that the metabasites are
91 alkali-basalts, which may have originated in either a rift setting or as oceanic islands
92 (Stenberg, 2005). Unlike many other mafic rocks from southern Africa, the Wilgenhoutsdrif
93 shows no geochemical subduction signature. The mafic and at least partly submarine
94 volcanism, together with the presence of minor serpentinites in the sequence leads to the
95 suggestion of an oceanic tectonic setting prior to its involvement in the Namaqua collision.
96 We analysed detrital zircons to investigate if the sediments had a juvenile character, reflecting
97 an oceanic setting, or formed close to an old crustal source.

98 *Fig. 3*

99

100 Although ascribed by most workers to the early stages of the Namaqua Wilson Cycle,
101 previous dates for the Wilgenhoutsdrif Group, summarised in Table 1 have not been
102 consistent. A felsic volcanic rock dated at 1290 ± 8 Ma (Moen, unpublished data) in Cornell
103 et al. (2006), establishing an age for the volcanism in this Group.

104

105 Two samples were analysed from sedimentary units within the Wilgenhoutsdrif Group. The
106 outcrop displayed quartzite and calcsilicate layers interbedded with conglomerate. The U-Pb
107 data for these detrital zircons are concordant (Fig. 4b), and shown as Pb-Pb data in a
108 probability density plot in Fig. 4a, range between 1770 and 2864 Ma, with the major
109 population between 1800 and 2200 Ma.

110 *Fig. 4*

111

112 **Koras Group**

113 The Koras Group (Fig. 2) overlies highly deformed units, including the Wilgenhoutsdrif
114 Group. As shown in Fig. 3, it is made up of two bimodal volcanic sequences comprising
115 basalt, rhyolite and sediments like conglomerate and sandstone. Each sequence represents a
116 cycle of bimodal volcanism and sedimentation. It is situated in fault basins and considered to
117 be related to a trans-tensional setting (Grobler et al., 1977), developed during late to post-
118 collision. The Koras Group is usually described as undeformed, although in many samples
119 greenschist facies mineral assemblages pseudomorph the magmatic minerals. Most previous
120 workers agreed that the entire Koras Group postdated Namaqua deformation in the entire
121 region. However, Sanderson-Damstra (1982) documented deformation fabrics in the
122 Bossienek Formation, meter-scale folds as well as slickenside striations in outcrops of
123 micaceous sandstone, which we also observed. His mapping also established the existence of
124 gentle folding in the lower Swartkopsleege rhyolites, identified two phases parallel to the

125 regional FN2 and FN3 (FN3 crosscutting FN2) respectively and an angular unconformity
126 between them and the overlying Rouxville basalts on the farm Karos Settlement. In this work
127 four different units were sampled within the Koras Group. They are described in stratigraphic
128 order from base to top. The Swartkopsleegte rhyolite is from the first cycle and recently
129 yielded an ion probe Pb-Pb age of 1171 ± 7 Ma (Gutzmer et al., 2000). Our sample contained
130 a small number of zircons, which for 21 spots yield a discordia upper intercept age of $1163 \pm$
131 12 , and for the 9 concordant grains a concordia age at 1173 ± 12 Ma (Table 2, Fig. 5a). The
132 concordia age is interpreted as the age of extrusion. The lower intercept of 328 ± 25 Ma
133 reflects an ancient lead loss event during the Carboniferous, possibly corresponding to the
134 Dwyka glaciation in the Gondwana continent. Much of the present land surface in this area is
135 an exhumed Dwyka surface and tillite occurrences are common.

136 *Fig. 5*

137

138 Two rhyolitic lava samples were taken from the Leeuwdraai Formation in the upper volcanic
139 cycle, which overlies the unconformity. The massive appearance of this formation led to its
140 interpretation as an intrusion by some workers. However, the occurrence of horizons of
141 welded tuff and layers with quartz-filled vesicles leave no doubt that it is an extrusive unit.
142 These two samples yielded plentiful zircon and concordia ages of 1095 ± 10 Ma by SHRIMP,
143 and 1092 ± 9 Ma by Nordsim respectively (Table 2, Fig. 5 b,c). The mean of these two ages,
144 which overlap statistically, is 1093 ± 7 Ma.

145

146 A unit regarded as a Swartkopsleegte correlate on the farm Ezelfontein in the southern
147 domain, 20 km south of the type area, was dated. This yielded a date of 1104 ± 8 Ma (Table 2,
148 Fig. 5d), showing that it is actually a Leeuwdraai correlate. Xenocrystic zircon cores in this
149 sample (DC0420) yield Pb-Pb ages from 1182 Ma to 2116 Ma old. Concerning the

150 correlations in the Koras Group, our sample is not the same as the Ezelfontein Formation
151 palaeomagnetic sample of Briden et al (1979). Their sample is from a basaltic unit today
152 referred to as Boom River Formation.

153

154 The uppermost Kalkpunt Formation red sandstone sample gave a wide range of detrital zircon
155 U-Pb ages from 1116 up to 1897 Ma (Table 2, Fig. 5e). This reflects the ages in the
156 provenance area towards the end of Koras volcanism. It suggests that the volcanism was not
157 so extensive that it covered the whole area, although it is possible that the 1900 Ma grains
158 were xenocrysts in Koras lavas. This sandstone has been used to define a paleomagnetic pole
159 with age given as 800-1050 Ma (Briden et al., 1979) and taken as 1065 Ma (Weil et al.,
160 1998). Field relationships suggest that the volcanic rubble which forms the base of this
161 sedimentary unit was deposited soon after the 1093 ± 7 Ma Leeuwdraai Formation volcanism
162 ceased, thereby establishing a maximum and probably true age for the Kalkpunt Sandstone
163 Formation.

164

165 **Blauwbosch and Rooiputs intrusives**

166 The Blauwbosch granite and the Rooiputs granophyre have been interpreted as intrusive and
167 extrusive or sub-volcanic equivalents of the Koras Group respectively, based on their lack of
168 deformation and the similarity in geochemical signatures (Geringer and Botha, 1976; Moen,
169 1987). They crop out 50 km and 38 km NW of Upington, respectively (Figs. 1 and 2). The
170 coarse-grained, two-feldspar Blauwbosch granite yielded a concordia age of 1093 ± 11 Ma
171 (Table 2, Fig. 5f). The Rooiputs granophyre is characterized by large numbers of mafic
172 xenoliths, reflecting bimodal magmatism, and gave a concordia age of 1093 ± 10 Ma (Table
173 2, Fig. 5g). These ages confirm the correlation, but only with the upper part of the Koras
174 Group. Two xenocrystic zircons in the Rooiputs granophyre yield Pb-Pb minimum ages of

175 1818 and 1742 Ma, possibly reflecting Kheis Province rocks at depth. Three other xenocrysts
176 have low Th/U ratios that probably indicate metamorphic zircon (Schersten et al., 2000)
177 which yield a concordia age of 1187 ± 11 Ma.

178 This corresponds to the first Koras volcanic cycle and might reflect a metamorphic event in
179 the bedrock at that time. Similar ages have been reported further west in the Namaqua
180 Province (Raith et al., 2003) and as shown in the following section.

181

182 **Areachap Group**

183 The Areachap Terrane lies west of the Kaaien Terrane (Figs. 1 and 2), comprising a package
184 of predominantly mafic to minor felsic metavolcanic rocks and metasediments which have the
185 geochemical signature of a subduction-related arc complex (Geringer et al., 1994). This
186 terrane has an amphibolite to granulite facies metamorphic overprint, which is generally much
187 higher grade than those to the east. However, the amphibolite grade stretches into the
188 westernmost quartzites of the Kaaien Terrane and their deformational histories are commonly
189 correlated (Stowe, 1986; van Zyl, 1981).

190

191 The Areachap Group was defined by Geringer and Botha (1984). It was conceived as a group
192 of subduction-related formations which were accreted to the Kalahari Craton during the
193 Namaqua orogeny (Fig. 2). Common features are the rock assemblages dominated by mafic
194 and intermediate metavolcanics and their erosion products, the geochemical subduction
195 signatures of the Copperton, Bokspuits and Jannelsepan mafic rocks and Besshi-type Cu-Zn
196 mineralization which has very similar Pb and S isotope signatures at Copperton and Areachap
197 Mines (Voet and King, 1986; Theart et al., 1989).

198 Its juvenile character was established by a Kober method zircon date of 1285 ± 14 Ma
199 (Cornell et al., 1990) at Copperton, 200 km south of Upington (Table 1). Views on this

200 correlation are not unanimous, some workers consider the Boven Rugseer Shear Zone (Fig.
201 2), which transects the two areas, a major terrane boundary which prohibits them from
202 correlating across it. Several strong geochemical similarities, Pb and S isotopes, Sm-Nd
203 model ages and zircon ages as well as lithology need to be explained if they are not
204 correlated. For further discussion see Cornell et al. (2006).

205 The narrow juvenile Areachap terrane seems to be unique in the Namaqua sector, but has
206 similar age and origin to the juvenile terranes in the Natal sector of the Province (Thomas et
207 al., 1994a). In this work, a metadacite was dated to establish ages for its origin and
208 metamorphism, as was a cordierite-biotite-quartz-sphalerite gneiss from the Areachap Mine,
209 close to Upington. The metadacite occurs as a thick migmatitic unit exposed in a quarry in the
210 largely metabasic Jannelsepan Formation. It contains extensive locally-derived leucosome
211 lenses and is also cut by tonalitic dykes which were folded after intrusion, showing that FN2
212 deformation accompanied migmatization. Conditions for performing hornblende barometry
213 based on the Al content were met, melt and fluid were present as were phases of K-feldspar,
214 titanite, plagioclase, magnetite, biotite, quartz and hornblende. The aluminium in hornblende
215 geobarometer gives pressures of 5-6 Kbar (Tindle and Webb, 1994), corresponding to 15-18
216 km depth for the migmatite (Table 3). Differences are due to different calibrations of the
217 barometer, the calibration of Schmidt (1992), gave 6.1-6.3 Kbar.

218 Zircons from this sample (DC0439), seen in backscattered electron images, exhibit
219 oscillatory-zoned magmatic cores related to the origin of the protolith. Most grains also have
220 thick rims or truncating overgrowths, which are ascribed to recrystallisation during
221 migmatization. The magmatic zircon gave a concordia age of 1241 ± 12 Ma (Table 2 and Fig.
222 6a) and the overgrowths, which have low (<0.1) Th/U ratios indicative of metamorphic zircon
223 gave a concordia age of 1165 ± 10 Ma (Table 2 and Fig. 6a). A borehole sample (AP15-825),
224 a cordierite-biotite-quartz-sphalerite gneiss from Areachap Mine north of the Orange river,

225 further confirms the regional extent of this metamorphic event. The sample has rare zircons
226 with metamorphic overgrowths yielding a concordia age of 1158 ± 12 Ma (Fig. 6b) as well as
227 monazites giving a mean Pb-Pb age of 1148 ± 12 Ma (Table 2).

228 *Table 3*

229 *Fig. 6*

230

231 **Swanartz Gneiss**

232 This granitic gneiss intervenes between the Areachap and the Wilgenhoutsdrif Group (Figs. 2
233 and 3). It is a generally coarse grained granitic gneiss with abundant biotite and hornblende as
234 well as K-feldspar porphyroblasts. It shows intrusive but generally bedding parallel
235 relationships to the surrounding schist of the Dagbreek Formation, although cross-cutting
236 contacts occur, with continuous structural fabric over them. Like many other granites in the
237 region, it is deformed and was thus classified as a pre- or syntectonic granite. It is also cut by
238 many bimodal Koras dykes. Its abundant zircon yields a concordia age of 1371 ± 9 Ma (Table
239 2, Fig. 5h), establishing that it formed early in the tectonic cycle and before the
240 Wilgenhoutsdrif Group was deposited.

241

242

243

244 **Discussion**

245

246 **Wilgenhoutsdrif Group**

247 The detrital zircon from metasedimentary samples of the Wilgenhoutsdrif Group shows that
248 most of the sediment was derived from an old provenance area. The 2.5 to 3.2 Ga zircons
249 were probably derived from the Kaapvaal Craton, but the main body of 1800-2100 grains is

250 more likely derived from the Kheis Province (Fig. 1) although the Craton does contain some
251 rocks of this age. Hills of sandstone and micaceous quartzite occur and the Hartley lava
252 horizon in the Kheis Front is dated at ~1929 Ma (Cornell et al., 1998). The Kheis Front is a
253 west-verging thrust package ramped over the Kaapvaal Craton, (Stowe, 1986), which may
254 reflect the closure of an ocean basin at the end of a 1.9 to 1.7 Ga Wilson cycle (Cornell et al.,
255 1998). As Eglington and Armstrong (2004) point out, the geochronological evidence for such
256 a tectonic cycle is fragmentary, however it seems to be the best explanation for the geological
257 relationships in the Kheis Province as shown in Fig. 2, which suggest a passive margin
258 development at 1.9 Ga and require a thrusting event before 1.7 Ga (Tinker et al., 2002).
259 Detrital zircons in the quartzites (Dagbreek Formation and Groblershoop Formation) to the
260 east and around the Koras and Wilgenhoutsdrif exposures also have ages that agree with the
261 dominating 1900-2200 Ma range, as well as a few older ages, (Moen, unpublished data), in
262 Cornell et al., (2006).

263

264 The chemical alteration trends and pillow structures in the mafic rocks together with the
265 occurrence of serpentinites and calcsilicate rocks in the Wilgenhoutsdrif Group point to an
266 oceanic setting. Together with the geochemical interpretation of an alkaline basalt protolith
267 (Stenberg, 2005), these data indicate that the Wilgenhoutsdrif Group originated in a
268 continental rift, accompanied by immature and locally shallow-water shelf sediments.

269

270 **Subduction and collision**

271 Some time after the onset of Wilgenhoutsdrif basin development, a subduction zone was
272 active in an ocean basin to the west, leading to arc magmatism in which Areachap mafic to
273 intermediate volcanic rocks formed between 1285 (Copperton Formation) and 1240 Ma
274 (Jannelsepan Formation). The geometry suggests that the Wilgenhoutsdrif Group formed in a

275 back-arc basin environment with the “Swanartz crustal block” on the outboard side. The
276 ocean basin closed and the terranes of the Namaqua Province were assembled by a series of
277 collisions, resulting in thickened crust and an extensive mountain belt across most of the
278 Province. The Areachap Terrane was thus juxtaposed onto the Kaaien Terrane and the
279 Wilgenhoutsdrif depositional basin was closed. This collision event was accompanied by
280 isoclinal deformation in rocks of both terranes, referred to as the main Namaqua deformation
281 event, FN2 (Humphreys and Van Bever Donker, 1987). After most orogenic deformation was
282 complete in the Kaaien Terrane, trans-tensional stress opened up a new basin much as
283 proposed by Jacobs et al. (1993), but much earlier than the 1070 Ma they suggested, leading
284 to the first Koras bimodal volcanism at 1173 Ma.

285

286 **Age of the collision from different terranes**

287 In the Kaaien Terrane the collision-related orogeny is bracketed between the age of the
288 Wilgenhoutsdrif Group at 1290 Ma and the oldest Koras Group rhyolites at 1173 Ma.
289 However, the 1173 Ma rhyolites show traces of folding as pointed out by Sanderson-Damstra
290 (1982) and so the FN2 deformation probably still affected this area to some extent, during the
291 first Koras volcanism. The collision event and subsequent deformation must have proceeded
292 for some tens of millions of years before deformation rates approached zero, thus the collision
293 probably began before 1200 Ma.

294 In the adjacent Areachap Terrane, arc-magmatic processes were active at 1240 Ma, but
295 migmatization at 15-18 km depth following the collision was in progress at 1165 Ma. At least
296 20 Ma was required for the build-up of heat, so the collision should have begun before 1185
297 Ma. Considering both terranes, the collision began after 1240 Ma and probably just before or
298 around 1200 Ma.

299

300 **End of tectonism in different terranes**

301 Our dating shows that while the lower Koras Group was being deposited in the Kaaien
302 Terrane at 1173 ± 12 Ma, the Jannelsepan Formation of the Areachap Group, today less than
303 12 km to the west, was subjected to migmatization and deformation in the Areachap Terrane
304 (1165 ± 10 Ma) in a syntectonic setting. This can be explained by the 15-18 km difference in
305 depth between the two localities, which prevailed at that time, according to our hornblende
306 barometry. The long-held concept that the Koras postdates all tectonism in the Namaqua
307 Sector of the Province (Barton and Burger, 1983; Gutzmer et al., 2000) must therefore be laid
308 to rest.

309

310 Four ion probe dates for Koras Group rhyolites suggest that there were two discrete pulses of
311 magmatism at 1173 and 1093 Ma. Both intrusive equivalents which we dated fall in the latter
312 group. We cannot exclude the possibility that all the zircons found in the two Swartkopsleepte
313 samples thus far dated by ion-probe are actually xenocrysts. However, we have had no
314 evidence to support this idea and consider it less likely.

315

316 The unconformity between the first and second volcanic cycles, recognised by Du Toit,
317 (1965) and documented by Sanderson-Damstra (1982) is now shown to represent an interval
318 of some 80 Ma (1173-1093). After 1093 Ma there is no sign of folding in the Koras Group,
319 although tilting continued. The Koras dykes and correlated intrusions which cut the Areachap
320 Terrane are also undeformed, which shows that tectonism in the Areachap Terrane had waned
321 by 1093 Ma. It seems likely that by this time the Areachap Terrane had been exhumed from
322 the mid-crustal depths envisaged during the migmatization process.

323

324 In the broader context, (Raith et al., 2003) documented high grade metamorphism at 1187 Ma
325 in the Bushmanland terrane, associated with extensive granite magmatism of the 1210-1180
326 Little Namaqualand Suite (Clifford et al., 2004; Robb et al., 1999). These rocks crop out
327 around 300-400 km west of the area we investigated and correlations of tectonic events has
328 not yet been established.

329

330 **Magmatic event around 1100 Ma**

331 Geochemical work has shown (Geringer and Botha, 1976; Moen, 1987) that rhyolite of the
332 Koras Group and the intrusive Blauwbosch granite and the Rooiputs granophyre are related
333 and display a potassium-enriched calc-alkaline trend. Our zircon data now confirms that these
334 intrusives are linked to the Koras Group, but only to the second volcanic pulse, around 1093
335 Ma. Moreover, these intrusive and extrusive rocks together suggest a 'post tectonic' bimodal
336 magmatic event at 1093 Ma in the eastern Namaqua Sector. To the west (1087 Ma
337 charnockite date (Barton and Burger, 1983)) and south (Copperton) (Cornell et al., 1992),
338 magmatic intrusions such as charnockites, and low-P, high-T metamorphic events have been
339 dated around 1080 Ma, which reflect the same regional thermal pulse. This may be broadly
340 related to the 1106 ± 2 Ma Umkundo Igneous Province (Hanson et al., 2004), defined by a
341 large number of mafic intrusions on the otherwise undeformed Kaapvaal and Zimbabwe
342 Cratons. 1109 Ma magmatism has also been recognised near the west coast by (Raith et al.,
343 2003). A mantle process of continental scale seems to have happened at this time. This might
344 be related to either a superplume (Hanson et al., 2004) or to mantle delamination suggested by
345 Gibson (1996) which could explain the changes in age, down to 1040 Ma in western
346 Namaqualand.

347

348

349 **Evidence for 1.9 Ga Kheis Province crust at depth.**

350 The xenocrysts in the Rooiputs granophyre and some of the extrusive rocks of the Koras
351 Group are thought to be derived from deeper in the crust. These range in age from 2.1 to 1.74
352 Ga, similar to the main group of Wilgenhoutsdrif detrital zircons which are considered to be
353 derived from the Kheis Province. It thus seems likely that the Kheis Province extends beneath
354 the Kaaian Terrane, which was thrust onto it during the Namaqua collision. This is consistent
355 with the gravity-defined boundary of the Namaqua Province lying west of the Kaaian Terrane
356 (Fig. 1). Both xenocrystic and detrital zircons in and around the Koras basin reflect
357 Palaeoproterozoic crustal growth, possibly in the Kheis Province. These crustal events are too
358 young to reflect basement of the Kaapvaal Craton to the east, and too old to belong to the
359 Areachap juvenile island arcs further west.

360 The Swanartz gneiss is wedged between faults in the Kaaian terrane and its 1371 Ma age
361 predates all other basement rocks reported so far in eastern Namaqualand. Comparable ages
362 are known from 1350 Ma granulites near Marydale (Humphreys and Cornell, 1989), from the
363 Awasib Mountain land, Namibia (Hoal and Heaman, 1995). They probably all reflect passive
364 margin processes at the beginning of the Namaqua Wilson cycle.

365

366 **Conclusions**

367

368

369 1. Two “pre-tectonic” units have been dated, which formed before the Namaqua Province was
370 assembled by collisions. These are the 1371 ± 9 Ma Swanartz Gneiss in the Kaaian Terrane
371 and the 1241 ± 12 Ma Jannelsepan Formation in the Areachap Terrane.

372

373 2. The Wilgenhoutsdrif Group sediments were strongly influenced by older continental
374 material, derived mainly from the Kheis Province. The bimodal character of the volcanic
375 rocks likewise indicates significant crustal input during their generation. The Wilgenhoutsdrif
376 Group probably formed in a continental back arc rift before becoming involved in Namaqua
377 collisions.

378

379 3. The collision event which assembled terranes in the eastern Namaqua Sector started some
380 time after 1230 Ma to allow for the formation of the Jannelsepan Formation at 1241 ± 12 Ma
381 and probably around 1200 Ma to allow for pressure and heat build up to result in
382 migmatitisation at 1165 ± 10 Ma in the Jannelsepan Formation of the Areachap Terrane.

383

384 4. Ages of two discrete bimodal volcanic cycles in the Koras Group and their related intrusive
385 equivalents, the Blauwbosch Granite and the Rooiputs Granophyre have been determined.
386 These rocks, which range from slightly folded to undeformed, overlie and intrude highly
387 folded rocks in the Namaqua Front.

388

389 5. The 1173 Ma date for the first Koras volcanic pulse marks the end of all but gentle FN2
390 folding in the Kaaien Terrane. However the nearby Areachap Terrane was experiencing
391 migmatization and severe FN2 deformation at around that time. Thus the regional
392 tectonostratigraphic implications of a long-sought after “correct” date for the Koras Group are
393 much less profound than has been envisaged.

394

395 6. The two cycles in the Koras Group may have different origins, considering the 80 Ma time
396 gap. The early sequence probably originated in a pull-apart basin due to post-collision strike-

397 slip movements. The late cycle reflects a continental-scale thermal process in the mantle such
398 as a superplume or lithospheric delamination process.

399

400 7. An issue raised with the new chronostratigraphy of the Koras Group is the importance of
401 complementing stratigraphic mapping with additional dating. A consequence is that the
402 integrity of the Koras Group might be questioned. The 80 Ma time gap and unconformity
403 between the pulses of magmatism in the Koras Group might invalidate its definition as a
404 Group.

405

406 8. Paleoproterozoic zircon xenocrysts found in the Koras extrusives and correlated intrusives
407 reflect a 1.8-2.0 Ma crust-forming event. They probably originate from sediments or tectonic
408 basement which formed on the margin of the Kaapvaal Craton during the Kheis tectonic cycle
409 and was overridden by the Kaaien terrane during the Namaquan collision.

410

411 9. By determining the age of the last volcanic cycle in the Koras Group, the Leeuwdraai
412 rhyolite at 1093 ± 7 Ma, we have also established the maximum age of the sedimentation in
413 the Kalkpunt sandstone. This constrains the age of the paleopole taken from this formation at
414 younger than but close to 1093 Ma (we propose 1090 ± 5 Ma). These new data will contribute
415 to the refinement of palaeomagnetic data for other formations of the Koras Group, and more
416 importantly to Apparent Polar Wander curves for the Kalahari Craton in paleomagnetic
417 reconstructions.

418

419 Acknowledgments

420

421 The unpublished thesis of C. Sanderson-Damstra (1982) provided an invaluable basis for our
422 fieldwork. The authors would also like to thank two reviewers for comments that greatly
423 improved the manuscript. Martin Whitehouse and the Nordsim team are gratefully
424 acknowledged. The NordSIM facility is supported by the research councils in Denmark
425 Norway and Sweden and the Geological Survey of Finland, together with the Swedish
426 Museum of Natural History. This is Nordsim contribution no. 183. The work of ÅP and DHC
427 was supported by Swedish Research Council Grant 621-2003-4274 to DHC. This paper is
428 TIGeR publication No. 15.

References:

- Barton, E.S. and Burger, A.J., 1983. Reconnaissance isotopic investigations in the Namaqua mobile belt and implications for Proterozoic crustal evolution - Upinton geotraverse. In: B.J.V. Botha (Editor), Geological Society of South Africa, Marshalltown. Spec. Publ. 10, 173-191.
- Botha, B.J.V., Grobler, N.J. and Burger, A.J., 1979. New U-Pb age-measurements on the Koras Group, Cape Province and its significance as a time-reference horizon in eastern Namaqualand. Transactions of the Geological Society of South Africa 82, 1-5.
- Briden, J.C., Duff, B.A. and Kroener, A., 1979. Palaeomagnetism of the Koras Group, northern Cape Province, South Africa. Precambrian Research 10, 43-57.
- Cahen, L. and Snelling, N.J., 1984. The geochronology and evolution of Africa. Oxford University Press, Oxford. pp. 512
- Clifford, T.N., Barton, E.S., Stern, R.A., Duchesne, J.C., 2004. U-Pb zircon calendar Namaquan (Grenville) crustal events in the granulite-facies terrane of the O'okiep copper district of South Africa. Journal of Petrology 45, 669-691.
- Cornell, D.H., Armstrong, R.A., Walraven, F., 1998. Geochronology of the Proterozoic Hartley basalt formation, South Africa; constraints on the Kheis tectogenesis and the Kaapvaal Craton's earliest Wilson cycle, Aspects of tensional magmatism. Pergamon, London-New York, International. 26, 5-27.
- Cornell, D.H., Humphreys, H., Theart, H.F.J., Scheepers, D.J., 1992. A collision-related pressure-temperature-time path for Prieska copper mine, Namaqua-Natal tectonic province, South Africa. Precambrian Research 59, 43-71.
- Cornell, D.H., Kroener, A., Humphreys, H., Griffin, G., 1990. Age of origin of the polymetamorphosed Copperton Formation, Namaqua-Natal Province, determined by single grain zircon Pb-Pb dating. South African Journal of Geology 93, 709-716.
- Cornell, D.H., Thomas, R.J., Gibson, R., Moen, H.F.G., Moore, J.M., Reid, D.L., 2006. Namaqua-Natal Province. In: M.R. Johnson, C.R. Anhaeuser and R.J. Thomas (Editors), Geology of South Africa. Geol. Soc. S. Afr. and Council Geoscience, Pretoria, pp. 325-379.
- Cummings, G.L., Richards, J.R., 1975. Ore lead ratios in a continuously changing Earth. Earth Planetary Science Letters 28: 155-171.
- Dalziel, I.W.D., Mosher, S. and Gahagan, L.M., 2000. Laurentia-Kalahari collision and the assembly of Rodinia. Journal of Geology 108, 499-513.
- Du Toit, M.C., 1965. Koras Formation. Unpubl MSc Thesis, University of Orange Free State, South Africa, Bloemfontein, pp 110.
- Eglington, B.M., Armstrong, R.A., 2004. The Kaapvaal Craton and adjacent orogens, Southern Africa; a geochronological database and overview of the geological development of the craton, Kaapvaal Craton. Bureau for Scientific Publications, Pretoria, South Africa, pp. 13-32.
- Frimmel, H.E., 2004. Formation of a Late Mesoproterozoic Supercontinent: The South Africa-East Antarctica connection. In: P.G. Eriksson (Editor), The Precambrian Earth: tempos and events. Elsevier, pp. 240-254.
- Geringer, G.J., Botha, B.J.V., 1976. The quartz porphyry-granite relation in rocks of the Koras Formation west of Upington in the Gordonia District. Transactions of the geological Society of South Africa 79, 58-60.

- Geringer, G.J., Botha, B.J.V., 1984. Amphibolites as indicators of Proterozoic subduction and calc-alkaline volcanism along the eastern margin of the Namaqua mobile belt, South Africa, Abstracts; 27th international geological congress. International, pp. 315-316.
- Geringer, G.J., Humphreys, H.C., Scheepers, D.J., 1994. Lithostratigraphy, protolithology, and tectonic setting of the Areachap Group along the eastern margin of the Namaqua mobile belt, South Africa. *South African Journal of Geology* 97, 78-100.
- Gibson, R.L., Robb, L.J., Kisters, A.F., Cawthorn, R.G., 1996. Regional setting and geological evolution of the Okiep Copper District, Namaqualand, South Africa. *South African Journal of Geology* 99, 107-120.
- Grobler, N.J., Botha, B.J.V., Smit, C.A., 1977. The tectonic setting of the Koras Group. *Transactions of the geological Society of South Africa* 80, 167-175.
- Gutzmer, J., Beukes, N.J., Pickard, A., Barley, M.E., 2000. 1170 Ma SHRIMP age for Koras Group bimodal volcanism, Northern Cape Province. *South African Journal of Geology* 103, 32-37.
- Hanson, R.E., Crowley, James L., Bowring, S.A., Ramezani J., Gose, W.A., Dalziel, I.W.D., Pancake J.A., Siedel E.K., Blenkinsop T. G., Mukwakwami, J., 2004. Coeval Large-Scale Magmatism in the Kalahari and Laurentian Cratons during Rodinia Assembly. *Science* 304, 1126 -1129.
- Hoal, B.G., 1993. The Proterozoic Sinclair Sequence in southern Namibia; intracratonic rift or active continental margin setting? *Precambrian Research* 63, 143-162.
- Hoal, B.G., Heaman, L.M., 1995. The Sinclair Sequence: U-Pb age constraints from the Awasib Mountain area. *Communications of the Geological Survey of South West Africa/Namibia* 10, 83-91.
- Humphreys, H.C., Cornell, D.H., 1989. Petrology and geochronology of low-pressure mafic granulites in the Marydale Group, South Africa. *Lithos* 22, 287-303.
- Humphreys, H.C., Van Bever Donker, J.M., 1987. Aspects of deformation along the Namaqua Province eastern boundary, Kenhardt District, South Africa. *Precambrian Research* 36, 39-63.
- Jacobs, J., Thomas, R.J., Weber, K., 1993. Accretion and indentation tectonics at the southern edge of the Kaapvaal Craton during the Kibaran (Grenville) Orogeny. *Geology* 21, 203-206.
- Kröner, A., 1977. The Sinclair aulacogen - a late Proterozoic volcano-sedimentary association along the Namib desert of Southern Namibia (SWA). 9th Colloquium on African Geology, Göttingen, pp. 127-129.
- Ludwig, K.R., 1991. Isoplot: a plotting and regression program for radiogenic-isotope data.
- Ludwig, K.R., 1998. On the treatment of concordant uranium-lead ages. *Geochimica et Cosmochimica Acta* 62, 665-676.
- Moen, H.F.G., 1987. The Koras Group and related intrusives north of Upington; a reinvestigation. Geological Survey of South Africa, Pretoria, South Africa. *Bulletin* 85, pp. 20.
- Moen, H.F.G., 1999. The Kheis tectonic subprovince, Southern Africa; a lithostratigraphic perspective. *South African Journal of Geology* 102, 27-42.
- Nelson, D.R., 1997. Compilation of SHRIMP U-Pb zircon geochronological data, Record. Western Australia Geological Survey, pp. 189.
- Raith, J.G., Cornell, D.H., Frimmel, H.E., De Beer, C.H., 2003. New insights into the geology of the Namaqua tectonic province, South Africa, from ion probe dating of detrital and metamorphic zircon. *Journal of Geology* 111, 347-366.
- Robb, L.J., Armstrong, R.A., Waters, D.J., 1999. The history of granulite-facies metamorphism and crustal growth from single zircon U-Pb geochronology; Namaqualand, South Africa. *Journal of Petrology* 40, 1747-1770.

- (SACS), South African Committee for Stratigraphy, 1980. Stratigraphy of South Africa. Part 1 Lithostratigraphy of the republic of South Africa, South West Africa/Namibia, and the Republics of Bophuthatswana, Transkei and Venda, Handbook 8. Geological Survey of South Africa, pp. 690.
- Sanderson-Damstra, C.G., 1982. Geology of the central and southern domains of the Koras Group, Northern Cape Province. Unpubl. MSc. Thesis, Rhodes University, Grahamstown, pp. 163.
- Schersten, A., Årebäck, H., Cornell, D., Hoskin, P., Åberg, A., Armstrong, R., 2000. Dating mafic-ultramafic intrusions by ion-microprobing contact-melt zircon; examples from SW Sweden. *Contributions to Mineralogy and Petrology* 139, 115-125.
- Schmidt, M.W., 1992. Amphibole composition in tonalite as a function of pressure; an experimental calibration of the Al-in-hornblende barometer. *Contributions to Mineralogy and Petrology* 110, 304-310.
- Stacey, J.S., Kramers, J.D., 1975. Approximation of terrestrial lead isotope evolution by a two-stage model. *Earth and Planetary Science Letters* 26, 207-221.
- Stenberg, S., 2005. The tectonic setting of the Namaqua sector rocks in the Upington area, South Africa: A geochemical study. Earth Sciences Centre B469. MSc. Thesis, Gothenburg University, Gothenburg. pp. 40.
- Stowe, C.W., 1986. Synthesis and interpretation of structures along the north-eastern boundary of the Namaqua tectonic province, South Africa. *Transactions of the Geological Society of South Africa* 89, 185-198.
- Theart, H.F.J., Cornell, D.H., Schade, J., 1989. Geochemistry and metamorphism of the Prieska Zn-Cu deposit, South Africa. *Economic Geology and the Bulletin of the Society of Economic Geologists* 84, 34-48.
- Thomas, R.J., Agenbacht, A.L.D., Cornell, D.H., Moore, J.M., 1994a. The Kibaran of Southern Africa: tectonic evolution and metallogeny. *Ore Geology Reviews* 9, 131-160.
- Thomas, R.J., Cornell, D.H., Moore, J.M., Jacobs, J., 1994b. Crustal evolution of the Namaqua-Natal metamorphic province, Southern Africa. *South African Journal of Geology* 97, 8-14.
- Thomas, R.J., de Beer, C.H., Bowring, S.A., 1996. A comparative study of the Mesoproterozoic late orogenic porphyritic granitoids of Southwest Namaqualand and Natal, South Africa, IGCP 348 (Mozambique and related belts). Pergamon, London-New York, International. pp. 485-508.
- Tindle, A.-G., Webb, P.-C., 1994. PROBE-AMPH; a spreadsheet program to classify microprobe-derived amphibole analysis. *Computers-and-Geosciences* 20, 1201-1228.
- Tinker, J., de, W.M.J., Grotzinger, J., 2002. Seismic stratigraphic constraints on Neoproterozoic-Paleoproterozoic evolution of the western margin of the Kaapvaal Craton, South Africa. *South African Journal of Geology* 105, 107-134.
- van Zyl, C.Z., 1981. Structural and metamorphic evolution in the transitional zone between craton and mobile belt, Upington Geotraverse. PhD Thesis, University of Cape Town, Cape Town, pp. 243.
- Voet, H.W., King, B.H., 1986. The Areachap copper-zinc deposit, Gordonia District. In: C.R. Annhaeusser and M. S (Editors), *Mineral deposits of Southern Africa*. Geological Society of South Africa, pp. 1529-1538.
- Weil, A.B., Van der Voo, R., Mac Niocaill, C., Meert, J.G., 1998. The Proterozoic supercontinent Rodinia; paleomagnetically derived reconstructions for 1100 to 800 Ma. *Earth and Planetary Science Letters* 154, 13-24.
- Whitehouse, M.J., Claesson, S., Sunde, T., Vestin, J., 1997. Ion microprobe U-Pb zircon geochronology and correlation of Archaean gneisses from the Lewisian Complex of

Gruinard Bay, northwestern Scotland. *Geochimica et Cosmochimica Acta* 61, 4429-4438.

Whitehouse, M.J., Kamber, B.S., Moorbath, S., 1999. Age significance of U-Th-Pb zircon data from early Archaean rocks of West Greenland; a reassessment based on combined ion-microprobe and imaging studies. *Chemical Geology* 160, 201-224.

Captions to Figures and Tables:

Fig. 1. Map of southern Africa.

Modified after Cornell et al, 2006. Shows the spatial relationship of the ~1.0 Ga Namaqua Province to the Kaapvaal Craton. The clearly defined geophysical boundary runs northwestward along the tectonic front zone, but departs from the craton margin at Marydale, where the ~1.8 Ga Kheis Province is interposed between them.

Fig. 2. Map of the investigated area.

Sample locations are shown as asterisks except for DC01139 that crop out off the map to the NW. Outcrops patterns of the Koras Group, the Wilgenhoutsdrif Group and the Areachap Group are shown, as well as major shear zones.

Fig. 3. A generalised section A-B showing the Koras Group and its tectonostratigraphic context.

The profile A-B is shown in Fig 2. Longitude and latitude for A = 28°38' 400, 21°18' 100, B = 28°22' 000, 21°57' 800. The section is drawn through the Central Domain of the Koras Group. Drawn from the SA Council for Geoscience 1:250 000 geological map 2820 Upington, stratigraphic nomenclature following (Moen, in prep), for earlier names used for palaeomagnetism see Table 1. Thicknesses are not to scale, and the dips of faults and shears are schematic.

Fig. 4. Provenance age plot.

(a) Detrital zircon ages in two metasedimentary samples of the Wilgenhoutsdrif Group shown as a probability density plot. Number of spots are 22 (n=22) in 22 zircons. (b) Concordia plot of data in (a).

Fig. 5. Concordia diagrams of (a) DC0380 (b) S03-10 (c) DC0263 (d) DC0420 (e) DC0411 (f) DC01139 (g) DC01138 (h) DC0428.

Fig. 6. (a). Concordia diagram of sample DC0439, Jannelsepan Formation, Areachap Group. Displays two age groups, of magmatic and metamorphic origin. (b) Concordia diagram of sample AP15-825, Jannelsepan Formation, Areachap Group.

Table 1. Literature age compilation. Table 1. Literature age compilation.

* the Florida Formation paleomagnetic pole (Briden et al., 1979), was derived from outcrops of the present Boom River Formation.

Table 2. Age calculations for U-Pb ion probe zircon data, unless otherwise stated, used in this work. Errors are given at 2 σ level, except where indicated by * (at 95% confidence level) and calculations ignoring decay constant errors. For full data see supplementary data and for concordia plots, see Fig. 4, 5, 6.

Table 3. SEM-EDS element analysis of hornblende in the Jannelsepan migmatite, Areachap Terrane (DC0439) thin section, for Al in hornblende barometry (see text).

Figure 1

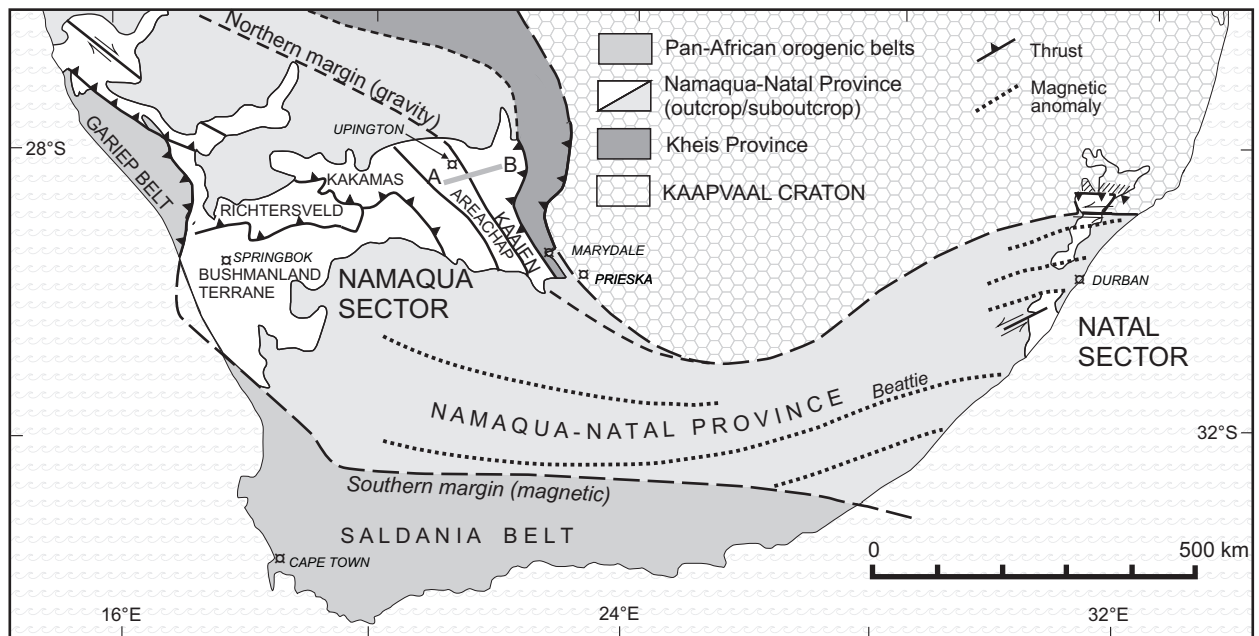


Figure 2

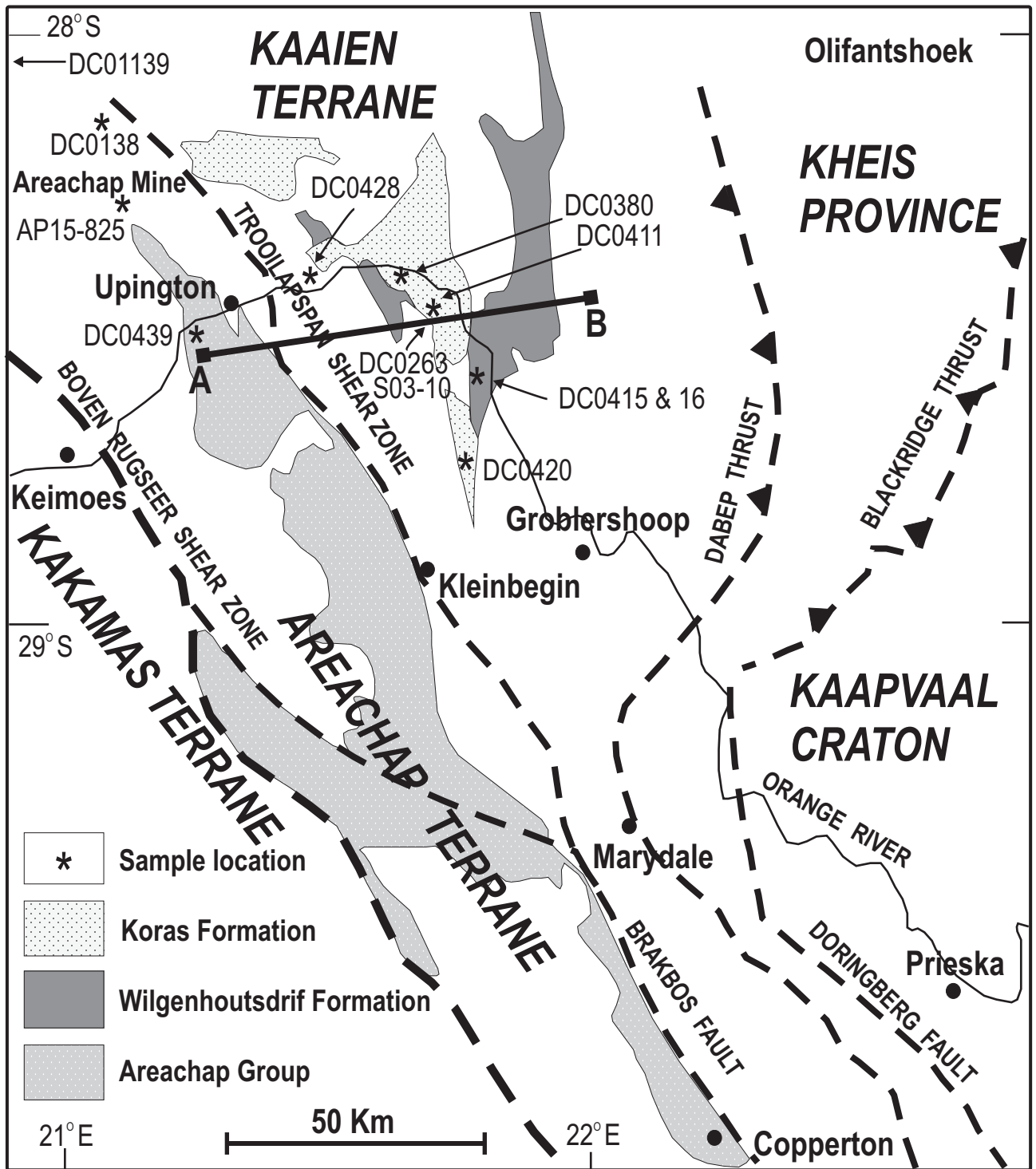


Figure 3

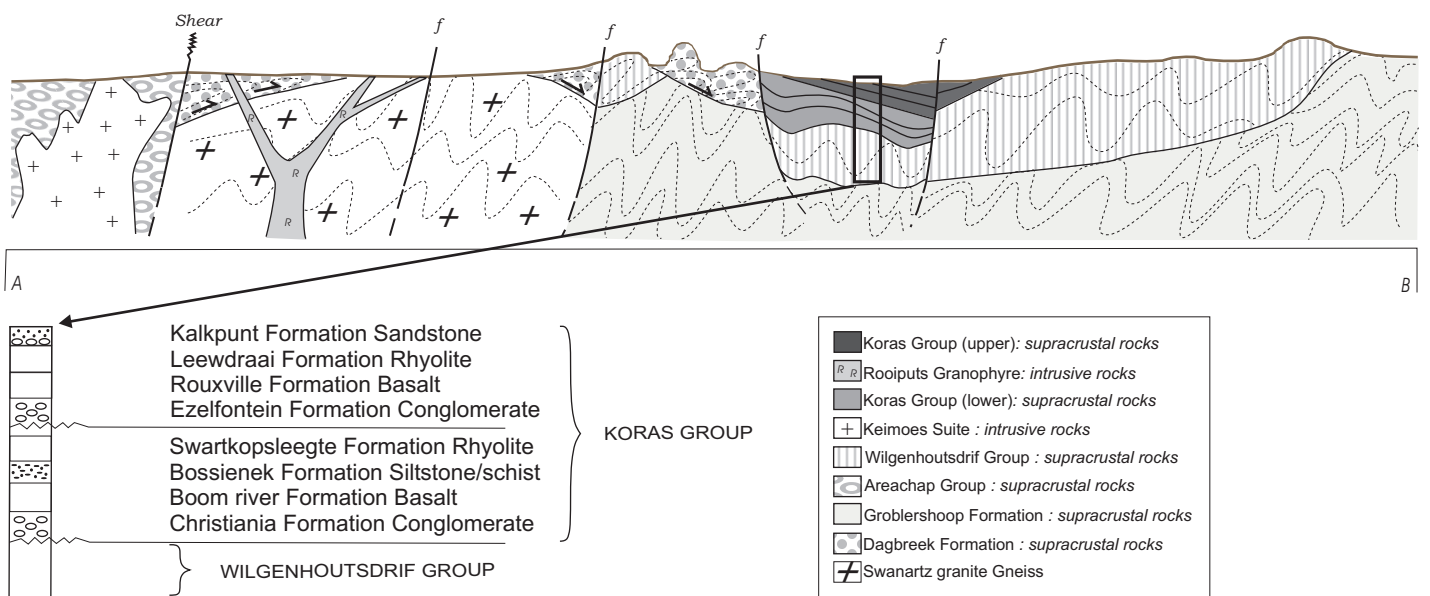


Figure 4

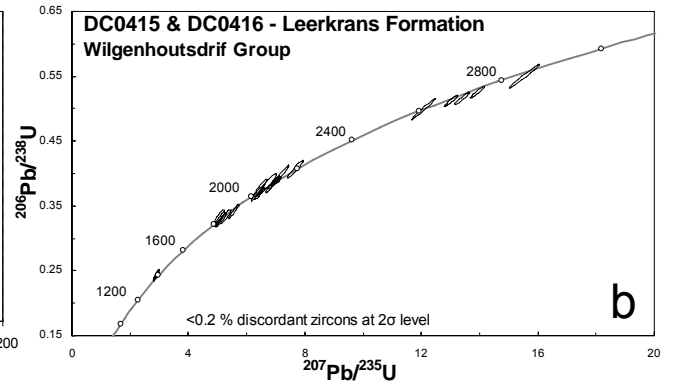
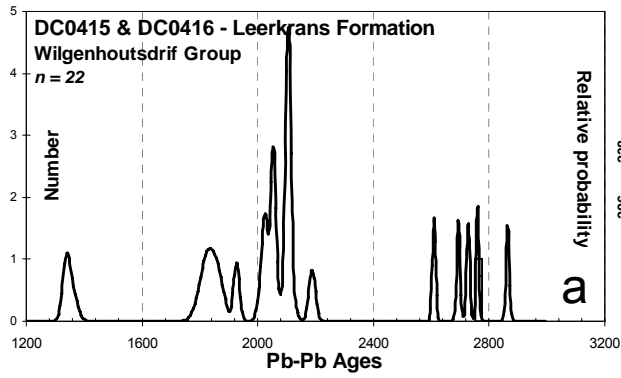


Figure 5

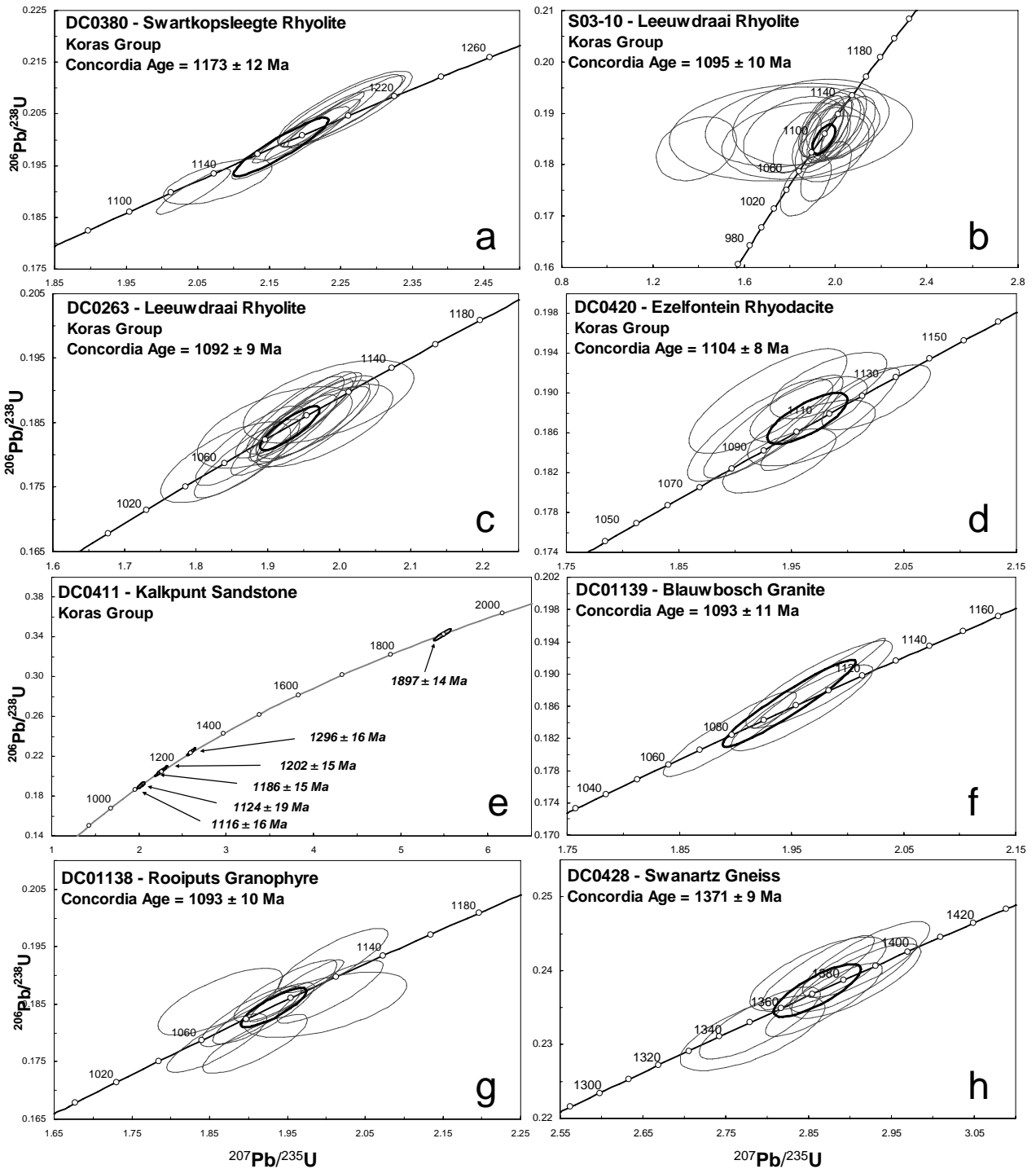


Figure 6

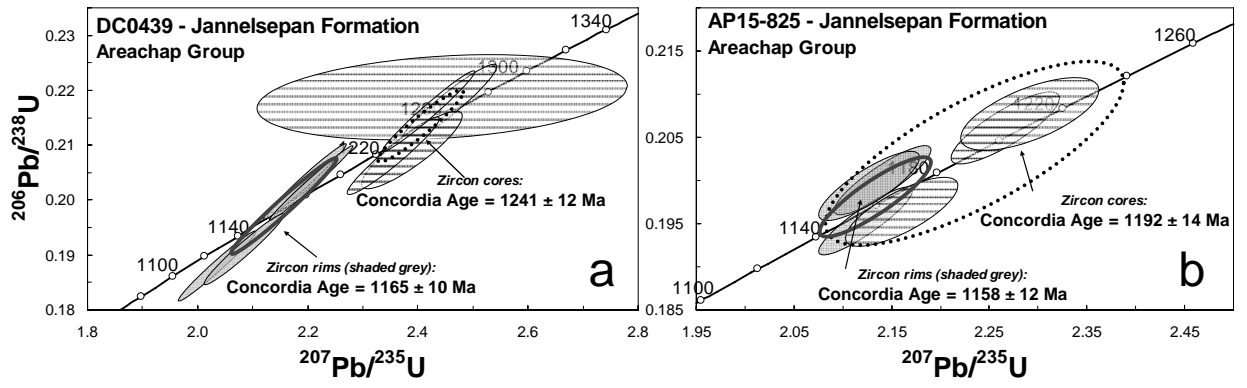


Table 1

	Rock type	Age $\pm 2\sigma$ (Ma)	Method, initial ratio	Reference
Koras Group extrusives				
Leeuwdraai Formation	Qtz porphyry lavas	1180 \pm 74	Discordia, 3 conventional U-Pb zircon samples	Botha et al., 1979
Swartkopsleegte Formation	Qtz porphyry lavas	1171 \pm 7	Weighted mean ion probe zircon Pb-Pb	Gutzmer et al., 2000
Swartkopsleegte Formation	Qtz porphyry lavas	1966 \pm 7	Ion probe zircon Pb-Pb one xenocryst in above sample.	Gutzmer et al., 2000
Boom River Formation, formerly Florida Formation*.	Basalts	1157 \pm 44 replaces 1176 \pm 18	Rb-Sr isochron, 7 points, MSWD 1.2, 0.7060 \pm 4	Recalculated data of Kröner, 1977
Koras intrusives				
Ezelfontein intrusion	Syenite	1076 \pm 52	Rb-Sr isochron 0.7065	Barton and Burger, 1983
Uitkoms dyke	Quartz porphyry	1032 & 1049	2 discordant conventional U-Pb zircon samples	Barton and Burger, 1983
Wilgenhoutsdrif Gp				
	Metabasic lava	1331 \pm 100	Rb-Sr isochron 0.7026	Barton and Burger, 1983
	Metabasic lava	1125 \pm 20	Rb-Sr errorchron 0.7017	Cornell 1975, in Cahen et al., 1984
	Acid lava	1336 & 1287	2 discordant conventional U-Pb zircon samples	Barton and Burger, 1983
Areachap Group				
Copperton Formation	Metadacite	1285 \pm 14	Kober method zircon Pb-Pb	Cornell et al., 1990
Jannelsepan Formation	Amphibolite	1300 to 1100	Imprecise Rb-Sr, Pb-Pb and Th-Pb data.	Barton and Burger, 1983

Table 2

<i>Sample</i>	<i>Formation, rock type</i>	<i>Age (Ma)</i>	<i>Type of grain</i>	<i>Spots used</i>	<i>Isoplot regression</i>	<i>MSWD</i>	<i>Th/U ratio</i>	<i>Lower intercept (Ma)</i>	<i>Location</i>	
									<i>S</i>	<i>E</i>
<i>Koras Group</i>										
DC0411	Kalkpunt, Sandstone	1116 ± 16	detrital	1	concordia	0.19	-		28°27.322′	21°40.348′
		1120-1196	detrital	5	Pb-Pb ages	-	-			
		1290	detrital	1	Pb-Pb ages	-	-			
		1824 & 1896	detrital	2	Pb-Pb ages	-	-			
DC0263	Leeuwdraai, Rhyolite	1092 ± 9	magmatic	14	concordia	0.47	>0.8		28°27.800′	21°40.800′
S03-10	Leeuwdraai, Rhyolite	1095 ± 10	magmatic	20	concordia	0.74	>0.8		28°28.204′	21°41.664′
DC0420	Rhyodacite at Ezelfontein (mapped as Swartkopsleegte)	1104 ± 8	magmatic	9	concordia	1.9	>0.7		28°37.894′	21°42.113′
		1182-1204	xenocrysts	3	Pb-Pb ages	-	-			
		1341	xenocryst	1	Pb-Pb age	-	-			
		1814-2117	xenocrysts	4	Pb-Pb ages	-	-			
DC0380	Swartkopsleegte, Rhyolite	1173 ± 12*	magmatic	9	concordia	0.75	0.08-0.57		28°24.878′	21°36.364′
		1163 ± 12	magmatic	21	discordia	1.6	-	328 ± 25		
<i>Wilgenhoutsdrif Group</i>										
DC0415	Leerkrans, Sandstone	2016 - 2760	detrital	9	Pb-Pb ages	-	-		28°29.757′	21°42.723′
DC0416	Leerkrans, Conglomerate	1337 - 2864	detrital	13	Pb-Pb ages	-	-		28°29.757′	21°42.723′
<i>Areachap Group</i>										
DC0439	Jannelsepan, Migmatite	1241 ± 12	magmatic	5	concordia	0.65	>0.75		28°30.279′	21°12.378′
		1165 ± 10*	metamorphic rim	5	concordia	0.67	<0.09			
AP15825	Jannelsepan, Biotite Gneiss	1192 ± 14	metamorphic?	3	concordia	<0,01	0.15-0.28		28°17.970′	21°02.500′
		1158 ± 12	metamorphic rim	3	concordia	1.7	<0.01			
		1142 ± 12	monazites	2	wtd mean Pb-Pb	2.6	-			
<i>Unit not assigned to a Group or Suite</i>										
DC0428	Swanartz Granite Gneiss	1371 ± 9	magmatic	8	concordia	0.12	>0.46		28°24.794′	21°25.900′
		1364 ± 13	magmatic	11	discordia	0.93	-	428 ± 120		
DC01139	Blauwbosch Granite	1093 ± 11	magmatic	4	concordia	1	>0.46		28°05.740′	20°49.044′
		1093 ± 11	magmatic	14	discordia	1.3	-	250 ± 39		
DC01138	Rooputs Granophyre	1093 ± 10	magmatic	10	concordia;	0.16	>0.2		28°08.891′	21°01.888′
		1818 & 1742	xenocrysts	2	Pb-Pb ages	-	-			
		1187 ± 14	xenocrysts	4	concordia	0.24	<0.06			

Table 3

Element	App Conc.	Intensity Corrn.	Weight%	Weight% Sigma	Atomic%	Compd%	Formula	Number of ions
<i>Analysis 1 - hornblende in DC0439</i>								
Na	0.76	0.69	1.1	0.05	1.16	1.48	Na ₂ O	0.45
Mg	3	0.65	4.6	0.06	4.6	7.62	MgO	1.79
Al	4.08	0.73	5.58	0.06	5.03	10.54	Al ₂ O ₃	1.96
Si	15.52	0.82	18.87	0.09	16.33	40.36	SiO ₂	6.35
K	1.25	1.06	1.18	0.03	0.73	1.42	K ₂ O	0.28
Ca	8.05	0.99	8.13	0.07	4.93	11.38	CaO	1.92
Ti	0.63	0.83	0.76	0.04	0.39	1.28	TiO ₂	0.15
Mn	0.65	0.83	0.78	0.05	0.35	1.01	MnO	0.13
Fe	14.29	0.85	16.84	0.13	7.33	21.66	FeO	2.85
O			38.92	0.16	59.14			23
Totals			96.76					
							Cation sum	15.89
<i>Analysis 2 - hornblende in DC0439</i>								
Na	0.72	0.69	1.05	0.05	1.11	1.41	Na ₂ O	0.43
Mg	3.02	0.65	4.64	0.06	4.64	7.69	MgO	1.8
Al	4.05	0.73	5.55	0.06	5.01	10.49	Al ₂ O ₃	1.95
Si	15.5	0.82	18.85	0.09	16.33	40.34	SiO ₂	6.35
K	1.2	1.06	1.14	0.03	0.71	1.37	K ₂ O	0.27
Ca	7.95	0.99	8.03	0.07	4.87	11.23	CaO	1.89
Ti	0.68	0.83	0.82	0.04	0.42	1.36	TiO ₂	0.16
Mn	0.64	0.83	0.77	0.05	0.34	0.99	MnO	0.13
Fe	14.46	0.85	17.04	0.14	7.42	21.92	FeO	2.88
O			38.92	0.16	59.17			23
Totals			96.8					
							Cation sum	15.87
<i>Analysis 3 - hornblende in DC0439</i>								
Na	0.7	0.69	1.01	0.05	1.07	1.36	Na ₂ O	0.42
Mg	2.99	0.65	4.58	0.06	4.58	7.6	MgO	1.78
Al	4.09	0.73	5.59	0.06	5.03	10.57	Al ₂ O ₃	1.96
Si	15.57	0.82	18.92	0.09	16.35	40.48	SiO ₂	6.36
K	1.25	1.06	1.18	0.03	0.74	1.43	K ₂ O	0.29
Ca	8.09	0.99	8.17	0.07	4.95	11.43	CaO	1.92
Ti	0.64	0.83	0.77	0.04	0.39	1.28	TiO ₂	0.15
Mn	0.66	0.83	0.8	0.05	0.35	1.03	MnO	0.14
Fe	14.37	0.85	16.94	0.14	7.36	21.79	FeO	2.86
O			39.01	0.16	59.18			23
Totals			96.98					
							Cation sum	15.87

Supplementary material for on-line publication

Sample/ spot	[U] ppm	[Th] ppm	Th/U meas.	$f_{206}\%$	$^{207}\text{Pb}/^{235}\text{U} \pm 1\sigma$ error	$^{206}\text{Pb}/^{238}\text{U} \pm 1\sigma$ error	Error corr.	Discordance (%)	$^{207}\text{Pb}/^{206}\text{Pb} \pm 1\sigma(\text{Ma})$	$^{206}\text{Pb}/^{238}\text{U} \pm 1\sigma(\text{Ma})$
DC01138 - Rooiputs Granophyre										
10a	132	114	0.869	0.71	1.8634 ± 2.8398	0.18549 ± 2.0720	0.73	9.4	1010 ± 39	1097 ± 21
10b	145	137	0.943	{0.08}	2.0085 ± 2.3101	0.19261 ± 1.9214	0.83	5.1	1085 ± 26	1136 ± 20
10c	137	123	0.895	{0.09}	2.0047 ± 2.2601	0.18717 ± 1.9109	0.85	-3.1	1139 ± 24	1106 ± 19
10d	139	124	0.889	0.16	1.9477 ± 2.2511	0.18731 ± 1.8968	0.84	2.7	1080 ± 24	1107 ± 19
17b	158	59	0.378	3.43	1.9978 ± 3.4824	0.18492 ± 2.0333	0.58	-5.8	1156 ± 55	1094 ± 20
20a	112	77	0.685	{0.17}	1.9027 ± 2.2390	0.18293 ± 1.8952	0.85	0.3	1080 ± 24	1083 ± 19
20b	113	77	0.689	{0.13}	1.9193 ± 2.2377	0.18340 ± 1.9264	0.86	-0.7	1092 ± 23	1086 ± 19
24a	103	67	0.655	{0.07}	1.9086 ± 2.3284	0.17811 ± 1.8956	0.81	-7.9	1140 ± 27	1057 ± 19
24b	106	70	0.664	{0.07}	1.8591 ± 2.2776	0.17821 ± 1.8953	0.83	-2.9	1086 ± 25	1057 ± 19
61a	349	72	0.207	{0.04}	1.9616 ± 2.0452	0.18733 ± 1.8955	0.93	1.3	1094 ± 15	1107 ± 19
17a*	462	27	0.058	0.06	2.2398 ± 1.9748	0.20443 ± 1.8987	0.96	1.4	1184 ± 11	1199 ± 21
64a*	391	23	0.059	{0.03}	2.2176 ± 1.7809	0.20223 ± 1.6486	0.93	0.2	1185 ± 13	1187 ± 18
62a	1075	6	0.005	2.89	1.5560 ± 2.2956	0.15061 ± 1.9055	0.83	-16.3	1067 ± 26	904 ± 16
47e	403	24	0.059	{0.04}	2.2061 ± 1.8035	0.20055 ± 1.6592	0.92	-1.2	1192 ± 14	1178 ± 18
30a	439	5	0.011	{0.00}	2.1121 ± 1.7579	0.19675 ± 1.6487	0.94	1.4	1143 ± 12	1158 ± 17
65a	113	111	0.980	{0.07}	5.5908 ± 1.8318	0.36478 ± 1.6491	0.90	11.9	1818 ± 14	2005 ± 28
69a	98	109	1.108	{0.04}	4.5445 ± 1.9836	0.30918 ± 1.7370	0.88	-0.4	1742 ± 17	1737 ± 26
72a	392	24	0.062	{0.03}	2.1869 ± 1.8291	0.19979 ± 1.6490	0.90	-0.7	1182 ± 16	1174 ± 18
DC01139 - Blauwbosch Granite										
19a	933	429	0.460	0.18	1.9744 ± 1.9891	0.18887 ± 1.9510	0.98	2.5	1090 ± 8	1115 ± 20
25a	110	132	1.208	{0.13}	1.9749 ± 2.1784	0.18869 ± 1.8951	0.87	2.2	1093 ± 21	1114 ± 19
6a	469	407	0.867	0.92	1.8948 ± 2.0624	0.18254 ± 1.8995	0.92	0.5	1076 ± 16	1081 ± 19
8a	240	191	0.795	0.35	1.9594 ± 2.1375	0.18580 ± 1.8952	0.89	-0.9	1108 ± 20	1099 ± 19
25b	78	90	1.150	{0.15}	1.9403 ± 2.4045	0.18299 ± 1.9958	0.83	-3.4	1119 ± 27	1083 ± 20
6b	621	353	0.568	0.39	1.7928 ± 2.0266	0.17383 ± 1.9401	0.96	-3.1	1063 ± 12	1033 ± 19
26a	54	64	1.180	{0.00}	1.9511 ± 2.3742	0.18233 ± 1.9113	0.81	-5.5	1137 ± 28	1080 ± 19
26b	340	261	0.767	3.21	1.6860 ± 2.7771	0.16678 ± 1.9488	0.70	-3.0	1023 ± 40	994 ± 18
47a	4124	2778	0.674	3.44	0.3789 ± 3.6886	0.04844 ± 1.8978	0.51	-37.5	482 ± 68	305 ± 6
47a2	3879	2670	0.688	7.77	0.4148 ± 5.5568	0.05115 ± 1.9197	0.35	-43.7	560 ± 110	322 ± 6
50a	441	414	0.938	0.38	1.7446 ±	0.16830 ± 1.9107	0.94	-7.1	1073 ± 14	1003 ± 18
63a	171	82	0.477	0.63	1.8521 ± 2.2849	0.17626 ± 1.8971	0.83	-5.3	1101 ± 25	1047 ± 18
63b	364	266	0.730	0.08	1.8255 ± 2.0143	0.17435 ± 1.8958	0.94	-5.7	1093 ± 14	1036 ± 18
63a	544	621	1.143	1.56	1.7620 ± 2.1983	0.16594 ± 1.8966	0.86	-12.7	1121 ± 22	990 ± 17
DC0263 - Leeuwdraai Rhyolite, Koras Group										
18a	47	66	1.392	0.98	1.9097 ± 3.7424	0.18427 ± 2.2666	0.61	1.8	1073 ± 59	1090 ± 23
20b	80	79	0.983	{0.15}	1.9851 ± 3.9651	0.18828 ± 2.2532	0.57	0.5	1107 ± 64	1112 ± 23
21a	122	98	0.803	{0.16}	1.9638 ± 2.6587	0.18434 ± 2.2532	0.85	-3.6	1128 ± 28	1091 ± 23
21b	50	46	0.931	{0.13}	1.9747 ± 3.3270	0.18454 ± 2.2677	0.68	-4.3	1137 ± 48	1092 ± 23
25b	53	51	0.951	{0.11}	1.9693 ± 2.8585	0.18584 ± 2.2663	0.79	-1.8	1117 ± 34	1099 ± 23
27a	130	107	0.819	{0.10}	1.8713 ± 2.6013	0.17942 ± 2.2495	0.86	-2.2	1086 ± 26	1064 ± 22
2a	133	113	0.846	{0.09}	1.9471 ± 2.5831	0.18651 ± 2.2610	0.88	1.5	1088 ± 25	1102 ± 23
37a	126	145	1.148	0.18	1.9313 ± 2.5830	0.18585 ± 2.2566	0.87	2.1	1078 ± 25	1099 ± 23
39a	94	92	0.986	{0.11}	1.9632 ± 2.6225	0.18521 ± 2.2479	0.86	-2.2	1118 ± 27	1095 ± 23
3a	187	168	0.900	{0.05}	1.9460 ± 2.4565	0.18539 ± 2.2587	0.92	-0.2	1098 ± 19	1096 ± 23
44a	69	102	1.482	0.30	1.8412 ± 3.2562	0.17887 ± 2.3183	0.71	0.2	1059 ± 45	1061 ± 23
4a	138	157	1.139	0.39	1.8744 ± 2.6516	0.18143 ± 2.2442	0.85	0.8	1067 ± 28	1075 ± 22
7a	216	222	1.029	{0.06}	1.9567 ± 2.4826	0.18637 ± 2.2801	0.92	0.3	1099 ± 20	1102 ± 23
9a	138	137	0.991	{0.13}	1.9224 ± 2.5415	0.18308 ± 2.2583	0.89	-1.5	1099 ± 23	1084 ± 23
44a	201	159	0.793	0.18	1.8741 ± 2.5455	0.17804 ± 2.3090	0.91	-4.7	1104 ± 21	1056 ± 23
44b	45	44	0.970	{0.32}	1.9322 ± 3.0643	0.17685 ± 2.2923	0.75	-11.8	1178 ± 40	1050 ± 22
20a	168	150	0.895	{0.10}	1.7820 ± 2.7874	0.16876 ± 2.4810	0.89	-10.2	1110 ± 25	1005 ± 23
25a	119	131	1.104	3.10	1.4685 ± 4.4927	0.18913 ± 2.2483	0.50	153.0	465 ± 84	1117 ± 23
29a	156	151	0.967	0.32	1.7824 ± 2.7931	0.17590 ± 2.3843	0.85	1.8	1028 ± 29	1045 ± 23
38a	75	92	1.218	0.54	1.8255 ± 3.0642	0.18127 ± 2.2956	0.75	6.3	1015 ± 41	1074 ± 23
DC0380 - Swartkopsleegte Rhyolite, Koras Group										
7a	524	47	0.090	0.40	2.2578 ± 2.4076	0.20545 ± 2.2491	0.93	1.4	1190 ± 17	1205 ± 25
8a	458	34	0.075	{0.01}	2.2218 ± 2.3256	0.20297 ± 2.2467	0.97	0.9	1182 ± 12	1191 ± 24
9a	267	31	0.116	{0.03}	2.2493 ± 2.5620	0.20559 ± 2.2494	0.88	2.3	1181 ± 24	1205 ± 25
9b	285	39	0.135	{0.00}	2.2557 ± 2.7565	0.20599 ± 2.3248	0.84	2.3	1183 ± 29	1207 ± 26
9c	208	44	0.213	{0.06}	2.1797 ± 2.4854	0.19941 ± 2.3071	0.93	-0.6	1179 ± 18	1172 ± 25
10a	392	141	0.359	{0.05}	2.2049 ± 2.3342	0.20237 ± 2.2448	0.96	1.4	1173 ± 13	1188 ± 24
14a	690	257	0.372	0.21	2.2233 ± 1.5917	0.20314 ± 1.5070	0.95	1.0	1182 ± 10	1192 ± 16
25b	67	38	0.571	0.75	2.0780 ± 2.4082	0.19190 ± 1.5063	0.63	-2.7	1160 ± 37	1132 ± 16
27b	966	437	0.452	1.47	2.0442 ± 1.6678	0.18998 ± 1.5090	0.90	-2.5	1148 ± 14	1121 ± 16
4a	508	193	0.380	0.06	2.2690 ± 2.3266	0.21013 ± 2.2481	0.97	7.1	1155 ± 12	1230 ± 25
44a	295	90	0.307	0.67	1.9820 ± 2.5222	0.18523 ± 2.2436	0.89	-4.0	1137 ± 23	1095 ± 23
43a	800	395	0.494	0.05	2.3038 ± 2.3769	0.21017 ± 2.2457	0.94	4.2	1185 ± 15	1230 ± 25
20a	896	298	0.332	0.05	2.2839 ± 2.3544	0.20977 ± 2.2579	0.96	5.3	1171 ± 13	1228 ± 25
24a	3196	1195	0.374	8.52	0.5098 ± 2.9022	0.06253 ± 2.2766	0.78	-32.6	572 ± 39	391 ± 9
43a	622	191	0.307	0.05	2.4896 ± 2.3916	0.22713 ± 2.2612	0.95	12.6	1185 ± 15	1319 ± 27
24a	1652	701	0.424	0.08	2.3103 ± 2.3039	0.21154 ± 2.2632	0.98	5.6	1177 ± 9	1237 ± 26
21a	278	110	0.394	{0.06}	2.1592 ± 2.5975	0.19492 ± 2.4901	0.96	-5.2	1205 ± 14	1148 ± 26
25a	154	168	1.090	0.13	2.1836 ± 1.8465	0.20298 ± 1.5064	0.82	4.2	1147 ± 21	1191 ± 16
26a	2392	472	0.198	2.93	1.2132 ± 1.7154	0.12296 ± 1.5115	0.88	-24.6	974 ± 16	748 ± 11
24b	1460	571	0.391	2.42	1.6811 ± 1.7400	0.16183 ± 1.5114	0.87	-11.1	1078 ± 17	967 ± 14
28a	1259	475	0.378	1.24	1.6758 ± 1.6449	0.15947 ± 1.5135	0.92	-14.3	1101 ± 13	954 ± 13
42a	388	65	0.166	0.22	2.2662 ± 1.6754	0.21226 ± 1.5063	0.90	10.5	1132 ± 15	1241 ± 17
DC0411 - Sandstone, Kalkpunt Formation, Koras Group										
7a	254	143	0.562	{0.03}	2.0043 ± 1.2708	0.18963 ± 1.1495	0.90	0.7	1112 ± 11	1119 ± 12
22a	173	136	0.788	0.08	5.4796 ± 1.2219	0.34242 ± 1.1450	0.94	0.1	1896 ± 8	1898 ± 19
24a	283	24	0.084	{0.03}	2.2809 ± 1.2476	0.20680 ± 1.1456	0.92	1.4	1197 ± 10	1212 ± 13
32a	292	42	0.144	{0.05}	2.2259 ± 1.2394	0.20325 ± 1.1456	0.92	0.9	1183 ± 9	1193 ± 12
46a	108	97	0.900	{0.11}	2.0259 ± 1.4116	0.19098 ± 1.1482	0.81	0.7	1120 ± 16	1127 ± 12
50a	217	181	0.832	{0.07}	2.5983 ± 1.2562	0.22461 ± 1.1449	0.91	1.4	1290 ± 10	1306 ± 14
9a	365	363	0.995	1.94	4.0226 ± 1.4581	0.26157 ± 1.2731	0.87	-20.0	1825 ± 13	1498 ± 17
23a	1141	101	0.088	2.04	1.8858 ± 1.7855	0.17355 ± 1.3315	0.75	-12.6	1167 ± 23	1032 ± 13
26a	456	30	0.067	3.07	1.6870 ± 1.6179	0.15665 ± 1.1888	0.73	-19.8	1150 ± 22	938 ± 10
63a	103	118	1.143	5.46	3.6994 ± 18.4155	0.52933 ± 2.2668	0.12	1379.1	227 ± 375	2739 ± 51

Sample/spot	[U] ppm	[Th] ppm	Th/U meas.	$f_{206}\%$	$^{207}\text{Pb}/^{235}\text{U} \pm 1\sigma$	$^{206}\text{Pb}/^{238}\text{U} \pm 1\sigma$	Error	Discordance	$^{207}\text{Pb}/^{206}\text{Pb} \pm 1\sigma(\text{Ma})$	$^{206}\text{Pb}/^{238}\text{U} \pm 1\sigma(\text{Ma})$
					error	error	corr.	(%)		
DC0415 - Quartzite, Leerkrans Formation, Wilgenhoutsdrif Group										
3a	238	138	0.578	1.31	6.4683 ± 2.4412	0.37790 ± 2.3299	0.95	2.9	2017 ± 13	2066 ± 41
13a	165	88	0.532	0.09	13.9303 ± 1.1605	0.52597 ± 1.1202	0.97	-1.6	2760 ± 5	2724 ± 25
15a	220	232	1.058	{0.04}	6.9786 ± 1.1562	0.38680 ± 1.1033	0.95	-0.1	2109 ± 6	2108 ± 20
18a	194	114	0.586	0.07	6.8605 ± 1.1684	0.38252 ± 1.1001	0.94	-0.6	2099 ± 7	2088 ± 20
17a	120	49	0.408	{0.04}	13.0256 ± 1.1632	0.51202 ± 1.1070	0.95	-1.3	2694 ± 6	2665 ± 24
26a	160	137	0.854	0.08	6.5050 ± 1.2288	0.37145 ± 1.1552	0.94	-1.2	2057 ± 7	2036 ± 20
26b	170	137	0.807	0.23	6.3926 ± 1.2106	0.36635 ± 1.1238	0.93	-2.2	2051 ± 8	2012 ± 19
28a	53	29	0.549	{0.15}	7.0073 ± 1.5105	0.38833 ± 1.2136	0.80	0.3	2110 ± 16	2115 ± 22
32a	134	66	0.497	0.08	13.4038 ± 1.2363	0.51611 ± 1.1853	0.96	-2.0	2728 ± 6	2683 ± 26
4a	141	67	0.474	0.43	6.1140 ± 2.5333	0.35066 ± 2.4442	0.96	-6.3	2049 ± 12	1938 ± 41
6a	694	402	0.580	3.99	3.4911 ± 1.2456	0.10134 ± 1.1347	0.91	-84.1	3184 ± 8	622 ± 7
6a	405	227	0.560	0.35	5.1259 ± 1.3717	0.30034 ± 1.3352	0.97	-18.0	2011 ± 6	1693 ± 20
10a	311	244	0.785	1.64	5.0297 ± 1.6631	0.33647 ± 1.2275	0.74	6.3	1773 ± 20	1870 ± 20
16b	139	116	0.839	3.74	6.1752 ± 2.0018	0.34117 ± 1.1004	0.55	-12.1	2115 ± 29	1892 ± 18
32b	256	88	0.346	0.26	12.6146 ± 1.1983	0.48937 ± 1.1692	0.98	-6.6	2716 ± 4	2568 ± 25
44a	100	97	0.977	2.76	2.4865 ± 1.7355	0.14531 ± 1.2865	0.74	-60.4	2016 ± 21	875 ± 11
DC0416 - Conglomerate, Leerkrans Formation, Wilgenhoutsdrif Group										
4a	301	211	0.701	0.24	6.3663 ± 2.2477	0.36976 ± 2.1835	0.97	0.1	2027 ± 9	2028 ± 38
9a	169	135	0.803	0.34	5.0708 ± 2.3427	0.32981 ± 2.1833	0.93	0.8	1824 ± 15	1837 ± 35
13a	302	104	0.346	0.27	15.5326 ± 2.2156	0.55021 ± 2.1850	0.99	-1.7	2864 ± 6	2826 ± 50
20a	173	126	0.725	0.30	7.6810 ± 2.3032	0.40687 ± 2.2027	0.96	0.6	2189 ± 12	2201 ± 41
28a	109	311	2.847	0.61	5.0630 ± 2.4920	0.33294 ± 2.1988	0.88	3.1	1804 ± 21	1853 ± 36
29a	266	110	0.414	0.32	6.8816 ± 2.2548	0.38294 ± 2.1850	0.97	-0.7	2102 ± 10	2090 ± 39
30a	146	184	1.259	0.18	5.1196 ± 2.3368	0.32873 ± 2.1832	0.93	-0.9	1847 ± 15	1832 ± 35
31a	291	141	0.483	0.12	5.5571 ± 2.2525	0.34128 ± 2.1826	0.97	-2.1	1928 ± 10	1893 ± 36
32a	132	134	1.015	0.57	6.7814 ± 2.4117	0.38741 ± 2.1815	0.90	3.1	2056 ± 18	2111 ± 39
33a	364	360	0.988	0.21	7.2063 ± 2.2422	0.39958 ± 2.1821	0.97	3.3	2109 ± 9	2167 ± 40
51a	368	201	0.546	0.10	12.0762 ± 2.2083	0.49951 ± 2.1815	0.99	0.1	2609 ± 6	2612 ± 47
64a	154	94	0.610	0.52	5.2620 ± 2.3979	0.33350 ± 2.1816	0.91	-1.0	1871 ± 18	1855 ± 35
65b	261	122	0.467	0.50	2.9064 ± 2.3840	0.24285 ± 2.1829	0.92	3.7	1356 ± 18	1401 ± 28
66a	417	132	0.316	0.20	2.8947 ± 2.2784	0.24422 ± 2.1824	0.96	5.9	1337 ± 13	1409 ± 28
DC0420 - Rhyolite at Ezelfontein, Koras Group										
96a	55	57	1.037	{0.10}	1.9394 ± 1.7082	0.18319 ± 1.1633	0.68	-3.0	1116 ± 25	1084 ± 12
97a	55	105	1.898	{0.21}	1.9830 ± 1.7250	0.19078 ± 1.1509	0.67	4.7	1079 ± 26	1126 ± 12
102b	53	55	1.046	{0.15}	1.9654 ± 1.7523	0.18838 ± 1.1452	0.65	2.6	1086 ± 26	1113 ± 12
102c	71	81	1.137	{0.09}	2.0252 ± 1.5762	0.18960 ± 1.1450	0.73	-1.4	1133 ± 21	1119 ± 12
104b	81	59	0.735	0.79	1.9678 ± 1.9040	0.18600 ± 1.1745	0.62	-1.4	1114 ± 30	1100 ± 12
9a	81	121	1.497	{0.10}	1.9341 ± 2.1136	0.18664 ± 1.8318	0.87	3.1	1073 ± 21	1103 ± 19
11a	96	138	1.440	{0.07}	1.9844 ± 2.0394	0.18739 ± 1.8248	0.89	-0.9	1116 ± 18	1107 ± 19
45a	64	71	1.111	0.31	1.9221 ± 2.2224	0.18629 ± 1.8328	0.82	3.8	1064 ± 25	1101 ± 19
58a	49	50	1.019	{0.20}	1.9290 ± 2.3995	0.18924 ± 1.8335	0.76	8.1	1040 ± 31	1117 ± 19
94a	130	80	0.617	{0.04}	2.7849 ± 1.3255	0.23452 ± 1.1488	0.87	1.4	1341 ± 13	1358 ± 14
96b	94	114	1.215	{0.19}	1.8057 ± 1.8680	0.17341 ± 1.1606	0.62	-5.2	1082 ± 29	1031 ± 11
98b	48	44	0.934	{0.26}	1.8110 ± 2.0195	0.17154 ± 1.1449	0.57	-8.7	1110 ± 33	1021 ± 11
21a	480	317	0.660	0.03	7.1009 ± 1.1767	0.39195 ± 1.1533	0.98	0.8	2117 ± 4	2132 ± 21
23a	260	92	0.352	{0.04}	2.2164 ± 1.3009	0.20016 ± 1.1778	0.91	-2.6	1205 ± 11	1176 ± 13
33a	119	171	1.433	0.34	2.0229 ± 1.6637	0.19790 ± 1.1449	0.69	12.4	1045 ± 24	1164 ± 12
49a	50	59	1.165	0.63	2.0143 ± 2.0888	0.19557 ± 1.1562	0.55	9.4	1060 ± 35	1151 ± 12
50a	1237	77	0.062	0.09	5.7726 ± 1.1661	0.35239 ± 1.1555	0.99	0.5	1938 ± 3	1946 ± 19
60b	395	152	0.386	{0.01}	6.0576 ± 1.2169	0.35774 ± 1.1449	0.94	-1.5	1997 ± 7	1971 ± 19
66a	316	129	0.410	{0.02}	2.2230 ± 1.2693	0.20303 ± 1.1665	0.92	0.9	1182 ± 10	1192 ± 13
66b	86	66	0.762	3.92	1.5868 ± 3.7238	0.15101 ± 1.1479	0.31	-18.9	1101 ± 69	907 ± 10
6a	69	87	1.267	1.62	1.6732 ± 3.3383	0.18174 ± 1.8666	0.56	32.2	831 ± 57	1076 ± 19
99a	276	435	1.575	2.05	4.3393 ± 2.1082	0.28385 ± 1.5459	0.73	-12.6	1814 ± 26	1611 ± 22
102a	78	107	1.370	{0.20}	1.8370 ± 1.7232	0.17384 ± 1.1666	0.68	-7.7	1112 ± 25	1033 ± 11
36a	48	43	0.896	0.79	1.9073 ± 2.7362	0.18885 ± 1.9317	0.71	10.1	1021 ± 39	1115 ± 20
102d	85	111	1.307	{0.12}	2.0005 ± 2.1273	0.19428 ± 1.8349	0.86	8.7	1060 ± 22	1144 ± 19
104a	433	19	0.045	{0.02}	2.2118 ± 1.2628	0.20198 ± 1.1500	0.91	0.3	1183 ± 10	1186 ± 12
DC0428 - Swanartz Gte gneiss										
41a	109	84	0.773	{0.05}	2.9038 ± 1.7316	0.23945 ± 1.4098	0.81	0.2	1381 ± 19	1384 ± 18
32a	180	115	0.641	{0.03}	2.8609 ± 1.5864	0.23976 ± 1.3809	0.87	2.9	1350 ± 15	1385 ± 17
6a	257	159	0.619	0.67	2.7909 ± 1.7234	0.23291 ± 1.3882	0.81	-0.7	1358 ± 20	1350 ± 17
85a	113	109	0.963	{0.06}	2.9193 ± 1.7360	0.24149 ± 1.4083	0.81	1.5	1375 ± 19	1394 ± 18
76a	183	130	0.712	{0.02}	2.8684 ± 1.6274	0.23605 ± 1.3864	0.85	-1.5	1385 ± 16	1366 ± 17
101a	57	44	0.764	{0.15}	2.7822 ± 2.0783	0.23152 ± 1.4379	0.69	-1.7	1364 ± 29	1342 ± 17
118a	133	116	0.873	{0.07}	2.8612 ± 1.8943	0.23954 ± 1.3819	0.73	2.6	1352 ± 25	1384 ± 17
85b	146	67	0.456	{0.05}	2.9073 ± 1.7740	0.23859 ± 1.3953	0.79	-0.9	1391 ± 21	1379 ± 17
101b	315	220	0.700	0.05	2.9685 ± 1.4996	0.24795 ± 1.3726	0.92	5.8	1357 ± 12	1428 ± 18
100a	888	626	0.704	0.30	2.1901 ± 1.7972	0.18941 ± 1.7278	0.96	-14.4	1289 ± 10	1118 ± 18
148b	156	66	0.426	0.44	2.8148 ± 1.8069	0.24553 ± 1.3840	0.77	12.5	1273 ± 22	1415 ± 18
106a	282	130	0.460	{0.04}	2.9693 ± 1.7062	0.24613 ± 1.3773	0.81	3.8	1371 ± 19	1418 ± 18
73a	66	8	0.116	0.57	2.2911 ± 2.3488	0.19935 ± 1.5591	0.66	-9.1	1278 ± 34	1172 ± 17
41b	317	140	0.441	1.73	2.6340 ± 2.4107	0.25788 ± 1.4225	0.59	46.7	1044 ± 39	1479 ± 19
40a	649	270	0.417	1.82	2.3769 ± 1.7950	0.23178 ± 1.3705	0.76	30.8	1052 ± 23	1344 ± 17
106b	47	22	0.463	0.89	2.2294 ± 2.9844	0.20030 ± 1.5932	0.53	-3.4	1215 ± 49	1177 ± 17

Sample/ spot	[U] ppm	[Th] ppm	Th/U meas.	$f_{206}\%$	$^{207}\text{Pb}/^{235}\text{U} \pm 1\sigma$ error	$^{206}\text{Pb}/^{238}\text{U} \pm 1\sigma$ error	Error corr.	Discordance (%)	$^{207}\text{Pb}/^{206}\text{Pb}$ $\pm 1\sigma$ (Ma)	$^{206}\text{Pb}/^{238}\text{U}$ $\pm 1\sigma$ (Ma)
DC0439 - Migmatite, Jannelsepan Formation, Areachap Group										
4a	1072	797	0.744	2.00	2.4543 ± 2.3651	0.21729 ± 2.2280	0.94	2.1	1244 ± 15	1268 ± 26
40a	691	547	0.791	5.18	2.4434 ± 9.0795	0.21860 ± 2.3505	0.26	4.6	1223 ± 163	1274 ± 27
40b	758	649	0.856	4.18	2.3889 ± 2.5414	0.20904 ± 2.2272	0.88	-3.7	1266 ± 24	1224 ± 25
76a	1139	1003	0.881	1.90	2.3549 ± 2.3330	0.20798 ± 2.2271	0.95	-2.7	1248 ± 14	1218 ± 25
56a	1634	1466	0.897	0.78	2.4192 ± 2.2784	0.21605 ± 2.2261	0.98	3.1	1227 ± 10	1261 ± 26
4b*	1553	146	0.094	0.32	2.0348 ± 2.2702	0.18783 ± 2.2260	0.98	-4.8	1161 ± 9	1110 ± 23
12a*	1791	120	0.067	0.29	2.1947 ± 2.2641	0.20319 ± 2.2261	0.98	3.5	1156 ± 8	1192 ± 24
71a*	1706	19	0.011	0.12	2.2054 ± 2.2543	0.20299 ± 2.2260	0.99	2.3	1167 ± 7	1191 ± 24
75a*	1856	23	0.012	0.56	2.0838 ± 2.2960	0.19103 ± 2.2265	0.97	-4.5	1175 ± 11	1127 ± 23
115a*	1587	24	0.015	0.03	2.2062 ± 1.3357	0.20326 ± 1.3004	0.97	2.6	1165 ± 6	1193 ± 14
439a	1832	247	0.135	0.13	1.9409 ± 1.3388	0.17841 ± 1.2988	0.97	-10.3	1170 ± 6	1058 ± 13
2a	1904	35	0.018	0.25	1.5708 ± 2.3070	0.15049 ± 2.2315	0.97	-18.1	1087 ± 12	904 ± 19
2b	2902	86	0.030	4.74	0.6651 ± 2.6702	0.07273 ± 2.2260	0.83	-46.2	817 ± 31	453 ± 10
44a	1187	523	0.440	4.26	2.0737 ± 2.5156	0.18490 ± 2.2261	0.88	-12.0	1230 ± 23	1094 ± 22
39a	1962	33	0.017	0.20	1.5872 ± 2.2664	0.14950 ± 2.2260	0.98	-21.3	1121 ± 8	898 ± 19
406a	1930	28	0.015	0.05	1.4942 ± 1.3435	0.14061 ± 1.3001	0.97	-26.1	1123 ± 7	848 ± 10
405a	1755	18	0.010	0.16	2.0512 ± 1.3439	0.18785 ± 1.3016	0.97	-6.2	1177 ± 7	1110 ± 13
440a	2795	55	0.020	0.27	0.6587 ± 1.3938	0.07004 ± 1.3095	0.94	-51.8	875 ± 10	436 ± 6
63a	1502	32	0.021	0.87	1.6621 ± 2.3143	0.16255 ± 2.2261	0.96	-7.7	1046 ± 13	971 ± 20
53b	2986	54	0.018	0.20	0.6779 ± 2.2866	0.07126 ± 2.2267	0.97	-52.4	899 ± 11	444 ± 10
74b	1793	29	0.016	0.16	1.8825 ± 2.2853	0.17533 ± 2.2279	0.97	-9.7	1144 ± 10	1041 ± 21
75b	2522	2604	1.032	0.72	2.0624 ± 2.2598	0.18651 ± 2.2263	0.99	-9.0	1202 ± 8	1102 ± 23
84a	1572	29	0.019	0.17	2.2433 ± 2.2601	0.20783 ± 2.2260	0.98	6.0	1154 ± 8	1217 ± 25
AP15-825 - Biotite Gneiss, Jannelsepan Formation, Areachap Group										
2c	290	45	0.154	0.08	2.26659 ± 1.6072	0.2060 ± 1.3345	0.83	1.4	1192 ± 18	1208 ± 15
1b	200	32	0.160	0.08	2.16089 ± 1.7632	0.1963 ± 1.3341	0.76	-3.4	1193 ± 23	1155 ± 14
1c	183	51	0.276	0.08	2.29214 ± 2.0407	0.2076 ± 1.3349	0.65	1.5	1199 ± 30	1216 ± 15
1a*	434	3	0.007	{0.03}	2.12399 ± 1.4905	0.1952 ± 1.3321	0.89	-1.9	1170 ± 13	1150 ± 14
2a*	337	2	0.007	0.06	2.14116 ± 1.5220	0.2000 ± 1.3325	0.88	3.5	1138 ± 15	1175 ± 14
2b*	312	4	0.012	0.08	2.12787 ± 1.6041	0.1993 ± 1.3325	0.83	3.8	1132 ± 18	1172 ± 14
S03-10 - Rhyolite, Leeuwdraai Formation, Koras Group										
10.1	111	101	0.93	0.15	1.9578 ± 3.7529	0.1787 ± 2.1308	0.57	-10.4	1060 ± 21	1184 ± 61
10.2	63	60	0.97	0.63	1.9549 ± 3.9330	0.1877 ± 2.2090	0.56	2.4	1109 ± 23	1083 ± 65
10.3	63	51	0.83	0.81	1.8698 ± 3.9625	0.1759 ± 2.2011	0.56	-7.1	1044 ± 21	1124 ± 66
10.4	25	29	1.23	2.35	1.8274 ± 3.3010	0.1859 ± 2.6252	0.32	13.7	1099 ± 27	966 ± 161
10.5	302	370	1.27	0.17	2.0044 ± 2.3670	0.1869 ± 2.0118	0.85	-3.2	1104 ± 20	1141 ± 25
10.6	26	40	1.60	2.93	1.8118 ± 13.9696	0.1874 ± 2.7310	0.20	18.8	1107 ± 28	932 ± 281
10.7	29	27	0.96	2.24	1.8361 ± 12.0168	0.1846 ± 2.6426	0.22	10.4	1092 ± 27	990 ± 238
10.8	162	140	0.89	0.42	1.9565 ± 2.7856	0.1863 ± 2.0650	0.74	0.2	1101 ± 21	1099 ± 37
10.9	83	73	0.90	0.45	1.9428 ± 3.1082	0.1858 ± 2.1440	0.69	0.7	1099 ± 22	1091 ± 45
10.10	51	46	0.93	1.01	1.9852 ± 5.3844	0.1831 ± 2.3208	0.43	-6.8	1084 ± 23	1163 ± 96
10.11	93	87	0.96	0.53	2.0575 ± 3.7566	0.1872 ± 2.1511	0.57	-7	1106 ± 22	1190 ± 61
10.12	60	50	0.86	0.94	1.9384 ± 4.3568	0.1848 ± 2.2453	0.52	-0.3	1093 ± 23	1097 ± 75
10.13	65	61	0.97	0.70	2.0046 ± 4.3281	0.1886 ± 2.2151	0.51	-0.9	1114 ± 23	1124 ± 74
10.14	18	16	0.95	1.95	1.8919 ± 11.9583	0.1883 ± 2.9271	0.24	10.1	1112 ± 30	1010 ± 235
10.15	110	111	1.05	0.84	1.8328 ± 3.7869	0.1843 ± 2.1199	0.56	10.2	1090 ± 21	989 ± 64
10.16	78	118	1.58	3.33	1.3908 ± 8.3375	0.1831 ± 2.2259	0.27	160.7	1084 ± 22	416 ± 180
10.17	69	94	1.42	0.75	1.9896 ± 4.5524	0.1870 ± 2.2082	0.49	-1.8	1105 ± 22	1125 ± 79
10.18	13	17	1.31	4.62	1.8046 ± 19.5018	0.1863 ± 3.3567	0.17	17.7	1101 ± 34	935 ± 394
10.19	93	86	0.96	0.50	2.0031 ± 3.5426	0.1870 ± 2.1488	0.61	-3	1105 ± 22	1139 ± 56
10.2	107	95	0.91	0.42	1.9420 ± 3.3216	0.1874 ± 2.1254	0.64	3.2	1107 ± 22	1073 ± 51

Unmarked data has been used for a group, magmatic or detrital population
Data indicated by* has been used for a group, metamorphic rim/overgrowth population.
Crossed out spots/data has not been used in isoplot concordia calculations
For detrital samples (DC0411, DC0415, DC0416) crossed out spots are either non-concordant and
or they are duplicate spots from the same grain, and not represented in concordia or probability density plots, .
For sample DC01138 and DC0420 likely xenocrystic zircons are highlighted in their Pb-Pb age with bold text.
{} indicates values close to or below detection limit
Discordance in % was calculated from the ratio between the $^{206}\text{Pb}/^{238}\text{U}$ age over the $^{207}\text{Pb}/^{206}\text{Pb}$ age, not including errors,
where discordant data is given as negative values and reversed discordant spots as positive.